Available online at www.sciencedirect.com
ScienceDirect
Precambrian Research 155 (2007) 69–97
Precambrian Research
www.elsevier.com/locate/precamres

Geochemistry and zircon geochronology of the I-type high-K calc-alkaline and S-type granitoid rocks from southeastern Roraima, Brazil: Orosirian collisional magmatism evidence (1.97–1.96 Ga) in central portion of Guyana Shield

Marcelo E. Almeida [a,b,*], Moacir J.B. Macambira [b], Elma C. Oliveira [b]

[a] *CPRM-Geological Survey of Brazil, Av. André Araújo 2160, Aleixo, CEP 69060-001, Manaus, Amazonas, Brazil*
[b] *Isotope Geology Laboratory, Center of Geosciences, Federal University of Pará, CP 8608, CEP 66075-110, Belém, Pará, Brazil*

Received 13 August 2006; received in revised form 5 January 2007; accepted 16 January 2007

Abstract

The understanding of the geological evolution of the Uatumã-Anauá Domain in southeastern Roraima, central region of Guyana Shield, is of major significance in the study of the Amazonian craton. This region lies between some major Paleoproterozoic geological–geochronological provinces: Tapajós-Parima or Ventuari-Tapajos (dominant), Maroni-Itacaiúnas or Transamazon (northwest) and Central Amazonian or Central Amazon (southeast and east). Geological mapping of the northern area of Uatumã-Anauá Domain, integrated with whole rock geochemistry data and previous and new Pb-evaporation and U–Pb zircon geochronology, point out for a plutonic collisional magmatic event (1975–1968 Ma) represented by I-type high-K calc-alkaline (Martins Pereira) and S-type (Serra Dourada) granitoid rocks. This magmatism was probably generated from crustal sources by partial melting during amalgamation of the TTG-like Anauá magmatic arc (2028 Ma) with Transamazonian (2.2–2.0 Ga) and Central Amazonian (older than 2.3 Ga) terranes. Local cumulatic leucogranites fills planar structures of the Martins Pereira granites. These leucogranites show younger ages (1909 Ma) and several inherited zircons (2354, 2134, 1997 and 1959 Ma), suggesting origin from crustal sources.

Keywords: Paleoproterozoic; Granitoid rocks; Guyana Shield; Zircon geochronology; Geochemistry

1. Introduction

The Guyana Shield, with a surface area of nearly 1.5 million km^2, represents the northernmost section of the Amazonian craton. This shield was predominately formed during protracted periods of intense granitic magmatism, bracketed between 2.1 and 1.9 Ga (Fig. 1a and b). Despite representing an intricate component of the Amazonian craton, the Guyana Shield has seen only limited attention among the scientific community. Geological maps of the region are scarce (*e.g.* CPRM, 1999, 2000a; Delor et al., 2003), and only few petrographical, geochemical and geophysical studies are available. Comparison between previous studies from the Guyana Shield has been hampered by a lack of dependable age determinations, implying large errors (±50–100 Ma), which preclude any attempt to establish a fine chronology of the magmatic and metamorphic events.

The study area is concentrates on the central part of the Guyana Shield, in southeastern Roraima State

* Corresponding author. Tel.: +55 92 2126 0301; fax: +55 92 2126 0319.
E-mail address: marcelo_almeida@ma.cprm.gov.br (M.E. Almeida).

0301-9268/$ – see front matter © 2007 Elsevier B.V. All rights reserved.
doi:10.1016/j.precamres.2007.01.004

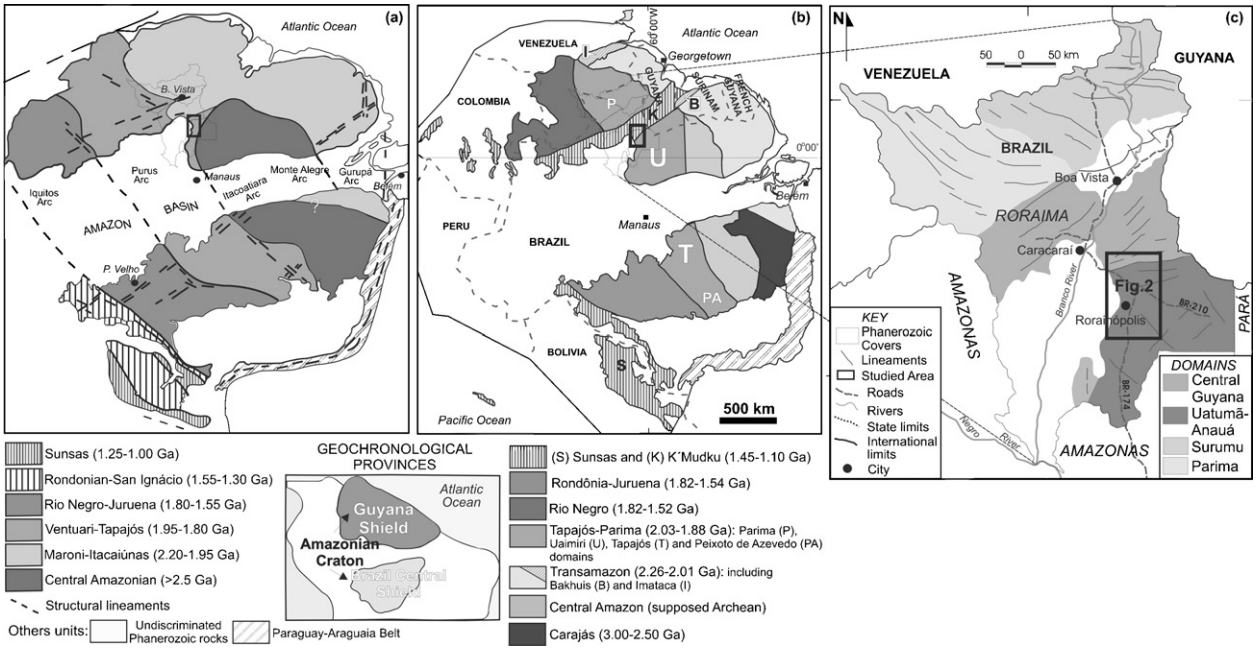

Fig. 1. The studied area location in Roraima State, plotted on the sketch maps of the Geochronological Provinces of the Amazonian craton according to (a) Tassinari and Macambira (1999, 2004) and (b) Santos et al. (2000, 2006), and on (c) the map of the lithostructural domains after Reis et al. (2003) modified by CPRM (2006).

(Brazil). Recent zircon geochronology data demonstrate that igneous rocks cropping out in this region (c. 4970 km^2, Fig. 2) show ages of 2.03 Ga (Faria et al., 2002) and 1.97–1.96 Ga (Almeida et al., 1997; CPRM, 2003), similar to the Tapajós Domain in Central Brazil Shield (Santos et al., 2000; Lamarão et al., 2002). However, the characteristics and significance of these events and ages are not fully understood (CPRM, 2000a; Almeida and Macambira, 2003). An example of this can be seen in the 2.03–1.96 Ga magmatic event which, unlike the 1.90 Ga calc-alkaline magmatism, is uncommon in other regions of the world. In addition the Tapajós Domain in Central Brazil Shield (southern Amazonian craton) and parts of the São Francisco Craton, Paleoproterozoic tectonic and magmatic activity between c. 2.0 and 1.9 Ga is recorded in Western Australia (Gascoigne Complex, Dalgaringa Supersuite, 2005–1970 Ma) by Sheppard et al. (2004) and southern Australia (Gawler Craton, Miltalie Gneiss, *ca.* 2000 Ma) by Daly et al. (1998). The Taltson Magmatic Zone of northern Canada (McDonough et al., 1993) and Kora-Karelian orogen of northern of Baltic Shield (Daly et al., 2001) also show 2.0–1.9 Ga magmatic events.

The aim of this paper is to provide new geochemical and geochronological constraints on the Martins Pereira and Serra Dourada granitoid rocks (Almeida et al., 2002). It is hoped that such studies will contribute to a better understanding of the lithostratigraphy, origin and geodynamic evolution of the northern part of the Uatumã-Anauá Domain, in the central portion of the Guyana Shield (Fig. 1). These data will be integrated with previous geochemical and geochronological data for other magmatic associations, mainly calc-alkaline granitoids older than 1.90 Ga. Particular focus will be placed on comparative geochemical and geochronology data from previous studies in the same region and from the southern part of the Amazonian craton.

2. Geological setting

Regional geological maps (CPRM, 2000a; Almeida et al., 2002) and zircon geochronological data (Almeida et al., 1997; Santos et al., 1997; Macambira et al., 2002; CPRM, 2003) have shown that Paleoproterozoic granitoid and volcanic rocks (1.97–1.81 Ga) are widespread in southeastern Roraima. These intrusive and extrusive rocks are emplaced within poorly exposed basement rocks that have maximum ages of around 2.03 Ga (Faria et al., 2002).

According to recent evolutionary models proposed for the Amazonian craton, the study area can be divided into several provinces. According to the work of Tassinari and Macambira (1999,2004), the study area

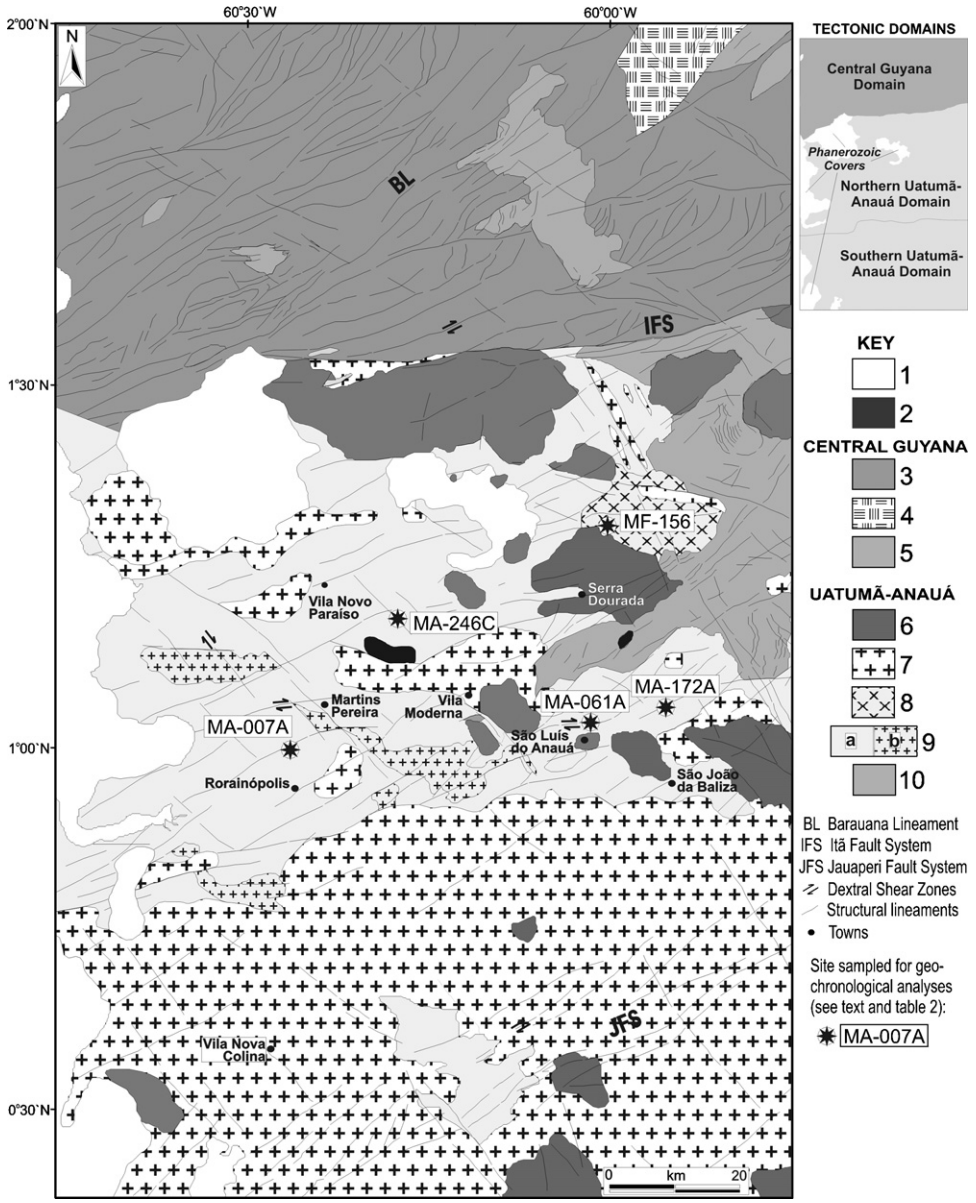

Fig. 2. Simplified geological map of Southeastern Roraima State modified from Almeida et al. (2002) and CPRM (2000a, 2005): (1) Plio-Pleistocene sedimentary covers; (2) Caracaraí Gabbro (1.52 Ga?); (3) Foliated granitoids (1.72 Ga), mylonitic granites (1.89 Ga), granulites, augen gneisses, metagranitoids and orthogneisses from Rio Urubu Complex (1.96–1.93 Ga); (4) S-type Curuxuim (garnet) Granite (1.97 Ga?); (5) Metavolcano-sedimentary sequence (Cauarane Group > 1.97 Ga); (6) (a) A-type Moderna (1.81 Ga) and Mapuera Granites (1.87 Ga), and minor enderbite and charno-enderbite (1.89 Ga); (7) Igarapé Azul and Caroebe Granites and minor volcanic rocks (1.90–1.89 Ga); (8) S-type Serra Dourada (cordierite) Granite (1.96 Ga); (9) High-K calc-alkaline granitoids with (a) normal to (b) high U, Th, K contents (Martins Pereira Granite, 1.97 Ga); (10) Metavolcano-sedimentary sequence (Cauarane Group related rocks; < 2.03 Ga?) and TTG calc-alkaline association (Anauá Complex, 2.03 Ga).

is largely enclosed in the Ventuari-Tapajós and Central Amazonian provinces, with a subordinate northeastern section falling within the Maroni-Itacaiúnas province. Santos et al. (2000, 2006) argue that all provinces were collectively affected by the K'Mudku Shear Belt in this same region (Fig. 1a and b). These authors conclude that Paleoproterozoic orogenic belts or magmatic arcs (*e.g.* Ventuari-Tapajós or Tapajós-Parima, and Maroni-Itacaiúnas or Transamazon provinces) accreted to the Archean craton with time and/or represent a set of rocks produced from melting of Archean crust (Fig. 1a and b; Cordani et al., 1979; Teixeira et al., 1989; Tassinari, 1996; Tassinari and Macambira, 1999, 2004; Santos et al., 2000, 2004, 2006).

The Tapajós-Parima (or Ventuari-Tapajós) Province is a Paleoproterozoic orogenic belt trends north–northwest and includes geological units which range from ~2.10 to 1.87 Ga in age (Santos et al., 2000, 2006; Tassinari and Macambira, 1999, 2004). This province was subdivided into four domains by Santos et al. (2000): Parima and Uaimiri, to the north, and Peixoto Azevedo and Tapajós, to the south. Southeastern Roraima belongs to the Uaimiri Domain. The Central Amazonian Province of the study area (Fig. 1a and b) display granitoid and volcanic rocks (1.88–1.70 Ga) lacking regional metamorphism and compressional folding (Santos et al., 2000; Tassinari and Macambira, 1999), and its basement is exposed scarcely. The age for this basement has been estimated via Nd-model ages at around 2.3–2.5 Ga (Tassinari and Macambira, 1999, 2004). According to these authors, the recorded Archean rocks in the Amazonian craton are only exposed in Imataca (Venezuela), Carajás and southern Amapá-northwestern Pará (Brazil). The Maroni-Itacaiúnas (or Transamazon) Province is also characterized by an orogenic belt with Rhyacian ages (2.25–2.00 Ga, Fig. 1a and b) and is correlated to the Birimian belt in West Africa (Tassinari and Macambira, 1999, 2004; Santos et al., 2000; Delor et al., 2003). The K'Mudku Shear Belt is characterized by low- to medium-grade mylonitic zones with *ca.* 1.20 Ga ages and cross-cuts the Rio Negro, Tapajós-Parima and Transamazon provinces, (Santos et al., 2000).

Taking into account lithological associations and geochronological data, Reis et al. (2003) and CPRM (2006), divided Roraima into four major domains—Surumu, Parima, Central Guyana and Uatumã-Anauá (Fig. 1c). Each of these domains contains a wide range of rock types and stratigraphic units. Southeastern Roraima is composed of the Central Guyana and Uatumã-Anauá lithostructural domains, that correspond to the K'Mudku Shear Belt and Uaimiri Domain, respectively (northern Tapajós-Parima Province) proposed by Santos et al. (2000).

The Central Guyana Domain (CGD) consists primarily of granulites, orthogneiss, mylonites and metagranitoids (Rio Urubu Metamorphic Suite) associated with low to high metamorphic grade metavolcanosedimentary covers (Cauarane Group) and S-type granite (Curuxuim Granite). The lineaments trend are strongly NE–SW trends (Figs. 1c and 2). The Uatumã-Anauá Domain (UAD) is characterized by E–W to NE–SW lineaments and the northern part of the domain Northern Uatumã-Anauá Domain shows an older metamorphic basement (Figs. 1 and 2) formed in a presumed island arc environment (Faria et al., 2002). This basement is composed of TTG-like metagranitoids to orthogneisses (Anauá Complex), enclosing meta-mafic to meta-ultramafic xenoliths, and is associated with some inliers of metavolcano–sedimentary rocks (Cauarane-like). The basement rocks are intruded by S-type (Serra Dourada Granite) and high-K, I-type calc-alkaline (Martins Pereira) granite plutons of c. 1.97–1.96 Ga (see zircon geochronology section).

In the southern area of the Uatumã-Anauá Domain, intrusive younger granites (with no regional deformation and metamorphism) are very common. The most prominent magmatism is related to the calc-alkaline Caroebe and Igarapé Azul granitoids (Água Branca Suite) with coeval Iricoumé volcanic rocks. Locally igneous charnockitic (Igarapé Tamandaré) and enderbitic (Santa Maria) plutons were also recorded. Several A-type granite bodies are widespread in the Uatumã-Anauá Domain (Fig. 2) represented by Moderna-Água Boa (1.81 Ga) and Mapuera-Abonari (1.87 Ga) granites.

3. Analytical procedures

3.1. Whole-rock geochemistry analysis

Whole-rock chemical analyses of 11 samples (milled under 200 mesh) were done at the Acme Analytical Laboratories Ltd. in Vancouver, British Columbia, Canada. The analytical package includes inductively coupled plasma-atomic emission spectrometer (ICP-AES) analyses after LiO_2 fusion for all major oxides (SiO_2, TiO_2, Al_2O_3, MnO, MgO, CaO, K_2O, Na_2O, P_2O_5) and LOI. Total iron concentration is expressed as Fe_2O_3. The trace elements were analyzed by inductively coupled plasma-mass spectrometer (ICP-MS), with rare-earth and incompatible elements determined from a $LiBO_2$ fusion and precious and base metals determined from an aqua regia digestion. Additional 16 samples were compiled (and partially reinterpreted) from CPRM (2000a). These last whole-rock chemical analyses were done at the Geosol Laboratories S.A., Belo Horizonte, Minas Gerais, Brazil.

3.2. Zircon isotope analysis

For isotope analysis, the zircon crystals were obtained from samples with 2–20 kg. After crushing (milled to 60–80 mesh) and sieving, heavy mineral fractions were obtained by water-mechanical and dense liquid concentrations, and processed under hand magnet and Frantz Isodynamic Separator. In order to remove impurities, zircon concentrates were washed with HNO_3 at 100 °C

(10 min), submitted to ultrasound cube (5 min) and finally washed on bidistilled H_2O. The less magnetic zircon concentrates (from five magnetic fractions) were preferred for hand-picking. Whenever possible only zircon grains free of alteration, metamictization features, inclusions and fractures were selected for analysis, however it was not always possible (see zircon descriptions below). All selected grains for analysis were photomicrographed *via* a conventional optical microscope.

Single-zircon dating by Pb-evaporation and U–Pb isotopic dilution in thermal ionization mass spectrometry (ID-TIMS) methods was performed at the Isotope Geology Laboratory (Pará-Iso), Federal University of Pará (UFPA), Brazil. The U decay constants are those recommended by Steiger and Jager (1977), and errors are given at the 95% confidence level. Ages of five samples were obtained by the Pb-evaporation technique established by Kober (1986, 1987), and only one sample was analyzed by U–Pb ID-TIMS. All isotope analyses were carried out on a Finnigan MAT 262 mass spectrometer in dynamic mode using the ion counting detector.

In the Pb-evaporation method on a single zircon, the selected grains were tied in Re-"evaporation"-filament and introduced in the mass spectrometer. The Pb was normally extracted from the crystals by heating in three evaporation steps at temperatures of 1450, 1500 and 1550 °C. The evaporated Pb was loaded on an "ionization" filament, which is heated for the isotope analyses. In this technique, the data were dynamically acquired using the ion counting system of the instrument. Pb signal was measured by peak hopping in the 206, 207, 208, 206, 207, 204 mass order along 10 scans, defining one block of data with 18 $^{207}Pb/^{206}Pb$ ratios. The $^{207}Pb/^{206}Pb$ ratio average of each step was based on five blocks or less, till the intensity beam was sufficiently high for a reliable analysis. Usually, the average $^{207}Pb/^{206}Pb$ ratio obtained in the highest temperature step was taken for age calculation, but the other steps are also considered. Outliers were eliminated using Dixon's test. The $^{207}Pb/^{206}Pb$ ratios were corrected for a mass discrimination factor of $0.12\% \pm 0.03\,amu^{-1}$, and results with $^{204}Pb/^{206}Pb$ ratios higher than 0.0004 were, in general, discarded. The ages were calculated with 2 sigma error and common Pb correction was done using appropriate age values derived from the two-stage model of Stacey and Kramers (1975). The obtained data were processed in shareware *Zircon* program (Scheller, 1998), DOS system version.

The Pb-evaporation on a single zircon method yields apparent $^{207}Pb/^{206}Pb$ ages and the degree of concordance of the analytical points is not possible to assess. Furthermore, zircon grains exhibiting a complex history, often yield mixed ages with no geological meaning (Dougherty-Page and Bartlett, 1999). With these uncertainties in mind, the age obtained for a single grain is considered as a minimum age. This being the case, as has been proposed in several studies (Kober, 1986; Andsell and Kyser, 1991; Macambira and Scheller, 1994; Söderlund, 1996), if a set of magmatic grains from the same sample yields similar ages, it is possible to suggest that such similarities indicate the time of the magmatic crystallization or episodic Pb loss.

The U–Pb ID-TIMS procedures undertaken in the Pará-Iso Laboratory followed those presented by Krymsky (2002). All zircon fractions selected for analysis were previously air abraded with pyrite crystals (20 mg and 0.1–0.5 mm diameter) in 1.2–1.8 psi pressure for 30–40 min. After abrasion the zircon grains were washed with HNO_3 and HCl (100 °C, 30 min) and H_2O-Millipore (3 times). The grains were then washed with methanol, weighed, spiked with $^{235}U–^{205}Pb$ tracer and dissolved with a mixture of HF and HCl in PTFE Teflon® bombs. Uranium and lead were separated with anion-exchange resin (Dowex® 1 × 8 200–400 mesh) in HCl medium in 50–70 μl columns. Uranium and Lead were loaded with Si-gel and H_3PO_4 (1N) onto the same out-gassed Re-filament and analyzed at 1400–1600 °C. For zircon analyses, blanks are <30 pg Pb and <1 pg U. The obtained data were processed in ISOPLOT/Excel program version 2 (Ludwig, 1999). The commom Pb interference was corrected using also the Stacey and Kramers (1975) model.

4. Whole-rock geochemical results

4.1. Major and minor oxides, and trace elements geochemistry

Analytical results of representative samples from Martins Pereira, Serra Dourada and Anauá granitoid rocks of the Northern Uatumã-Anauá Domain, including leucogranite blobs and lenses, are presented in Table 1 and plotted in diagrams in Figs. 3–7. Serra Dourada and Anauá results are extracted form CPRM (2000a). Creporizão (CPRM, 2000b) and Old São Jorge (Lamarão et al., 2002) granitoid rocks data from Tapajós region are also plotted in some diagrams for comparison with Martins Pereira granitoid rocks.

The Martins Pereira Granite consists of a compositionally wide series of rocks with SiO_2 contents between 49.3 and 74.6 wt.% (Table 1). The associated leucogranite pods and lenses have high SiO_2 contents (72.9–73.9 wt.%), but in the Harker diagrams show no correlation with the Martins Pereira Granite. For

Table 1
Chemical compositions of main plutonic associations of Northern Uatumã-Anauá Domain, such as Martins Pereira (meta)granitoid rocks, lenses and blobs of leucogranites, Serra Dourada granite and Anauá Complex

	Tonalites			Granodiorites and Monzogranites														Leucogranites		Granites		Enclave	TTG-like plutonic association			
Sample	MA-009B[1]	MA-176B[1]	MA-007C[1]	MF-011B[2]	MF-011A[2]	MA-246C1[1]	MA-172A[1]	MA-261B[1]	MA-119[1]	MA-061A[1]	PT-010[2]	MF-132A[2]	MA-007A[1]	RL-050[2]	RL-046[2]	MJ-213A[2]	RL-013[2]	PT-006A[2]	MA-246C2[1]	MA-007B[1]	MF-157[2]	MF-151[2]	MF-131B[2]	MF-129C[2]	MF-051B[2]	RL-116[2]	RL-119A[2]
Rock Type	bTnGn	bTn	ebTnGn	bMgr	bGd	mbTnGn	bMgrP	bMtGd	bMtMgr	bMtMgrP	bGd	mbMtMgr	bMtMgrP	bGd	bGd	bMgr	Mgr	bMgr	LcSgr	LcSgr	bMgr	mbSgr	aGbN	AMP	MtD	MtTn	MtTn
SiO_2 (wt. %)	49.33	55.91	60.04	62.85	63.52	64.55	65.16	66.91	68.03	68.23	68.24	68.72	68.87	70.95	71.14	73.96	74.33	74.60	72.92	73.92	70.30	71.70	41.30	50.20	52.50	59.40	59.80
TiO_2	2.71	1.11	1.15	0.86	0.80	0.88	0.86	0.72	0.40	0.78	0.56	0.39	0.78	0.28	0.28	0.22	0.22	0.19	0.08	0.06	0.41	0.31	2.00	2.60	0.90	0.77	0.61
Al_2O_3	12.44	17.09	16.05	15.61	15.27	15.96	14.71	14.13	15.25	13.38	15.06	15.66	13.55	15.42	15.46	13.70	14.66	13.89	14.42	14.15	14.30	14.50	14.00	12.00	22.00	17.00	18.90
Fe_2O_3*	20.96	8.61	7.01	7.50	7.96	5.76	5.70	5.27	2.96	4.87	5.73	3.78	4.23	2.66	2.68	2.26	1.92	2.20	0.49	0.50	3.87	2.99	19.87	18.74	7.90	6.26	3.27
MnO	0.22	0.15	0.13	0.16	0.15	0.15	0.10	0.10	0.07	0.09	0.14	0.08	0.08	0.10	0.10	0.06	0.06	0.10	0.02	0.01	0.07	0.07	0.29	0.36	0.11	0.13	0.12
MgO	2.42	2.77	2.78	3.14	2.22	1.84	1.48	1.30	1.05	1.36	1.62	1.01	1.03	0.60	0.52	0.44	0.36	0.36	0.15	0.07	0.94	0.66	8.60	4.50	2.60	3.10	2.00
CaO	5.66	6.07	5.54	3.65	3.74	2.39	3.00	2.56	3.12	2.55	2.73	2.22	2.59	2.42	2.22	1.21	1.53	1.51	0.85	1.17	1.50	0.77	10.10	8.70	7.20	5.30	5.50
Na_2O	2.54	3.91	3.47	2.94	3.24	2.70	2.70	2.80	3.05	2.79	2.73	3.44	2.81	3.73	3.84	2.82	3.46	3.12	2.07	2.37	2.90	2.50	1.50	2.20	5.20	3.20	4.40
K_2O	2.10	3.19	2.31	3.14	2.63	4.17	4.46	4.49	4.31	4.50	3.44	4.75	4.89	3.93	3.84	5.44	3.46	4.13	8.31	7.31	5.00	5.30	1.20	0.42	0.87	2.20	1.60
P_2O_5	1.31	1.19	0.39	0.14	0.26	0.30	0.47	0.37	0.20	0.38	0.13	0.22	0.38	0.10	0.11	0.03	0.07	0.05	0.06	0.01	0.10	0.17	0.33	0.22	0.32	0.21	0.32
LOI	0.10	0.90	0.70	0.95	0.87	1.10	1.10	0.90	0.90	0.90	0.58	0.64	0.60	0.42	0.47	0.28	0.21	0.38	0.80	0.60	0.33	0.67	0.65	0.01	0.33	0.45	0.23
TOTAL	99.79	100.90	99.57	100.95	100.67	99.80	99.74	99.55	99.34	99.83	100.95	100.92	99.81	100.60	100.67	100.42	100.29	100.54	100.17	100.17	99.72	99.64	99.84	99.95	99.93	98.02	96.75
Trace element (ppm)																											
Ni	21	16	26	-	-	26	14	12	7	20	-	-	20	-	-	-	-	-	2.11	2.61	-	-	-	31	5	14	5
Cr	821	-	753	-	-	547	274	342	68	274	-	-	342	-	-	-	-	-	205.26	68.42	-	-	-	138	34	90	48
Rb	184	97	183	296	280	228	307	282	157	233	186	191	187	140	149	216	153	169	192.92	229.09	204	414	32	11	53	83	36
Cs	5.72	0.91	8.50	-	-	4.98	14.60	13.68	6.40	8.10	9.10	2.53	6.10	2.52	2.53	2.52	7.13	10.07	1.01	2.01	9.0	9.0	2.5	-	36.0	2.5	2.5
Ba	563	1374	536	292	465	749	865	967	710	853	695	841	1025	952	1372	1217	959	961	1576.94	1807.77	684	373	460	75	908	679	757
Sr	456	683	494	176	327	284	200	199	298	180	225	291	217	544	517	290	448	277	313.58	246.16	203	103	272	123	1887	601	1221
Ga	31.30	25.86	25.59	13.18	12.14	26.72	22.81	23.42	17.57	20.40	17.19	16.17	18.70	11.09	5.05	5.04	5.09	5.03	12.28	13.46	12	20	16	-	31	19	19
Ta	2.51	0.71	1.82	2.50	2.50	1.12	1.52	1.72	0.81	1.60	2.50	2.50	1.70	2.50	2.50	2.50	2.50	2.50	0.20	0.20	2.50	2.50	5.00	-	12.00	2.50	2.50
Nb	32.50	17.95	26.90	14.19	16.18	21.74	25.14	19.56	9.24	23.20	13.14	12.13	23.40	11.09	12.13	8.06	7.13	10.07	2.21	2.21	9.0	28.0	12.0	17.0	5.0	2.5	10.0
Hf	33.70	19.98	9.20	20.00	20.00	11.48	16.32	10.75	9.24	11.30	20.00	20.00	10.90	20.00	20.00	20.00	20.00	20.00	2.31	2.91	-	-	-	-	-	-	-
Zr	1239	956	320	155	284	379	626	383	286	434	167	169	383	182	200	180	177	158	48.61	81.15	166	174	206	126	392	190	177
Y	120	44	48	25	22	50	69	52	28	47	30	19	60	13	6	12	14	4	82.62	5.82	47	56	31	33	22	19	19
Th	42	12	26	25	25	53	49	53	47	27	25	25	39	25	25	25	25	25	16.60	25.61	-	-	-	-	-	5.00	9.00
U	9	2	5	5	5	4	8	8	6	6	5	5	12	5	5	5	5	5	2.01	3.82	-	-	-	-	-	5.00	12.00
La	94.19	128.16	48.55	37.24	52.83	86.56	111.72	86.47	48.05	63.50	33.18	32.59	82.60	30.29	48.05	107.61	48.12	23.04	24.66	22.50	40.62	40.89	21.57	17.32	28.22	27.64	32.40
Ce	260.21	251.93	114.39	90.40	113.18	211.72	309.61	196.35	101.18	130.20	75.72	73.21	160.20	71.87	95.07	229.33	101.90	50.05	49.11	46.60	98.52	107.80	71.35	44.01	65.33	67.84	72.09
Pr	33.00	24.63	13.96	-	-	22.52	28.64	21.18	9.66	15.79	-	-	18.84	-	-	-	-	-	5.53	5.05	-	-	-	-	-	-	-
Nd	138.33	85.90	55.93	45.24	35.71	83.82	107.66	79.47	32.10	61.00	31.99	29.61	70.10	32.83	38.94	106.71	50.84	16.55	19.93	17.88	45.03	50.95	47.70	28.02	29.93	34.32	30.49
Sm	27.38	11.97	11.43	5.65	5.92	14.73	18.05	13.48	5.28	11.30	4.17	4.83	12.70	3.72	3.79	17.21	5.60	2.84	4.33	2.61	8.11	9.10	10.20	5.75	5.56	6.01	4.47
Eu	3.28	2.52	1.89	0.79	0.96	1.68	2.19	1.71	1.11	1.52	0.95	0.80	1.95	0.63	0.77	1.87	0.75	0.54	1.46	1.20	1.02	0.70	2.49	1.79	1.60	1.28	1.42
Gd	22.44	9.77	10.59	4.86	3.78	11.67	14.67	10.69	4.48	9.16	3.49	4.16	10.76	2.76	2.65	9.55	4.68	1.80	5.27	1.61	4.60	5.18	7.07	5.27	3.11	3.59	2.75
Tb	3.65	1.29	1.49	-	-	1.64	2.35	1.69	0.65	1.27	-	-	1.58	-	-	-	-	-	1.27	0.24	-	-	-	-	-	-	-
Dy	19.84	7.26	8.31	4.86	2.52	8.81	11.73	8.79	3.60	7.61	3.38	4.14	8.50	2.11	2.05	6.04	3.10	1.10	9.49	1.03	3.89	4.16	5.35	6.89	2.13	3.16	2.25
Ho	3.88	1.41	1.53	0.97	0.38	1.68	2.27	1.63	0.82	1.32	0.67	0.71	1.59	0.38	0.40	1.09	0.61	0.22	2.71	0.18	0.72	0.77	1.07	1.41	0.35	0.59	0.42
Er	11.75	4.15	4.66	2.63	0.94	4.86	6.69	4.39	2.23	4.29	1.77	1.79	4.89	0.85	0.99	2.37	1.58	0.55	10.71	0.65	1.61	1.76	2.90	3.94	0.80	1.37	0.96
Tm	1.86	0.59	0.69	-	-	0.72	0.99	0.64	0.42	0.58	-	-	0.72	-	-	-	-	-	2.04	0.09	-	-	-	-	-	-	-
Yb	12.28	4.08	4.23	1.83	0.80	4.65	6.10	3.70	2.38	4.16	1.07	1.08	4.94	0.63	0.85	1.37	1.72	0.41	14.13	0.62	0.97	1.18	1.82	3.20	0.60	1.04	0.79
Lu	1.85	0.70	0.65	0.22	0.14	0.79	0.99	0.58	0.43	0.58	0.16	0.12	0.71	0.09	0.11	0.18	0.23	0.08	2.48	0.10	0.14	0.16	0.27	0.35	0.09	0.12	0.09
ETR total	633.94	534.38	278.29	194.69	217.16	455.85	623.67	430.78	212.38	312.28	156.55	153.05	380.08	146.18	193.66	483.34	219.13	97.18	153.10	100.36	205.24	222.64	171.79	117.95	137.72	146.96	148.14
Mg#	18.61	38.91	43.99	45.34	35.64	38.75	33.96	32.82	41.26	35.61	35.85	34.64	32.53	30.71	27.96	27.95	26.82	24.58	37.74	21.71	32.50	30.41	46.16	32.23	43.73	38.77	36.54
Rb/Sr	0.40	0.14	0.37	1.68	0.86	0.80	1.54	1.42	0.53	1.29	0.83	0.66	0.86	0.26	0.29	0.74	0.34	0.61	0.62	0.93	1.00	4.02	0.12	0.09	0.03	0.14	0.03
Rb/Ba	0.33	0.07	0.34	1.01	0.60	0.30	0.36	0.29	0.22	0.27	0.27	0.23	0.18	0.15	0.11	0.18	0.16	0.18	0.12	0.13	3.35	0.90	14.38	6.82	17.13	8.18	21.03
Eu(n)/Eu*	0.39	0.69	0.52	0.45	0.58	0.38	0.4	0.42	0.68	0.44	0.74	0.53	0.5	0.58	0.71	0.41	0.44	0.68	0.93	1.66	0.47	0.29	0.85	0.98	1.07	0.78	1.15
(La/Sm)n	2.16	6.74	2.67	4.15	5.61	3.70	3.89	4.03	5.72	3.53	5.00	4.24	4.09	5.12	7.98	3.93	5.41	5.10	3.58	5.42	3.15	2.83	1.33	1.89	3.19	2.89	4.55
(Gd/Yb)n	1.47	1.93	2.02	2.14	3.83	2.02	1.94	2.33	8.31	1.78	2.62	3.11	1.76	3.51	2.52	5.62	2.20	3.56	0.3	2.08	3.82	3.55	3.13	1.33	4.18	2.79	2.82
(La/Yb)n	5.17	21.2	7.74	13.69	44.69	12.54	12.34	15.76	4.58	10.29	20.87	20.32	11.27	32.17	38.17	52.90	18.85	38.01	1.18	24.36	28.20	23.40	7.99	3.65	31.71	17.94	27.72

The geochemical data were obtained from this study[1] and CPRM (2000a)[2]. *Abbreviations*: a, amphibole; b, biotite; e, epidote; m, muscovite; D, diorite; Gb, gabbro; Gd, granodiorite; Mgr, monzogranite; N, norite; Sgr, syenogranite; Tn, tonalite; Gn, gneiss; Lc, leuco; Mt, meta; P, porphyritic; – , not available values.

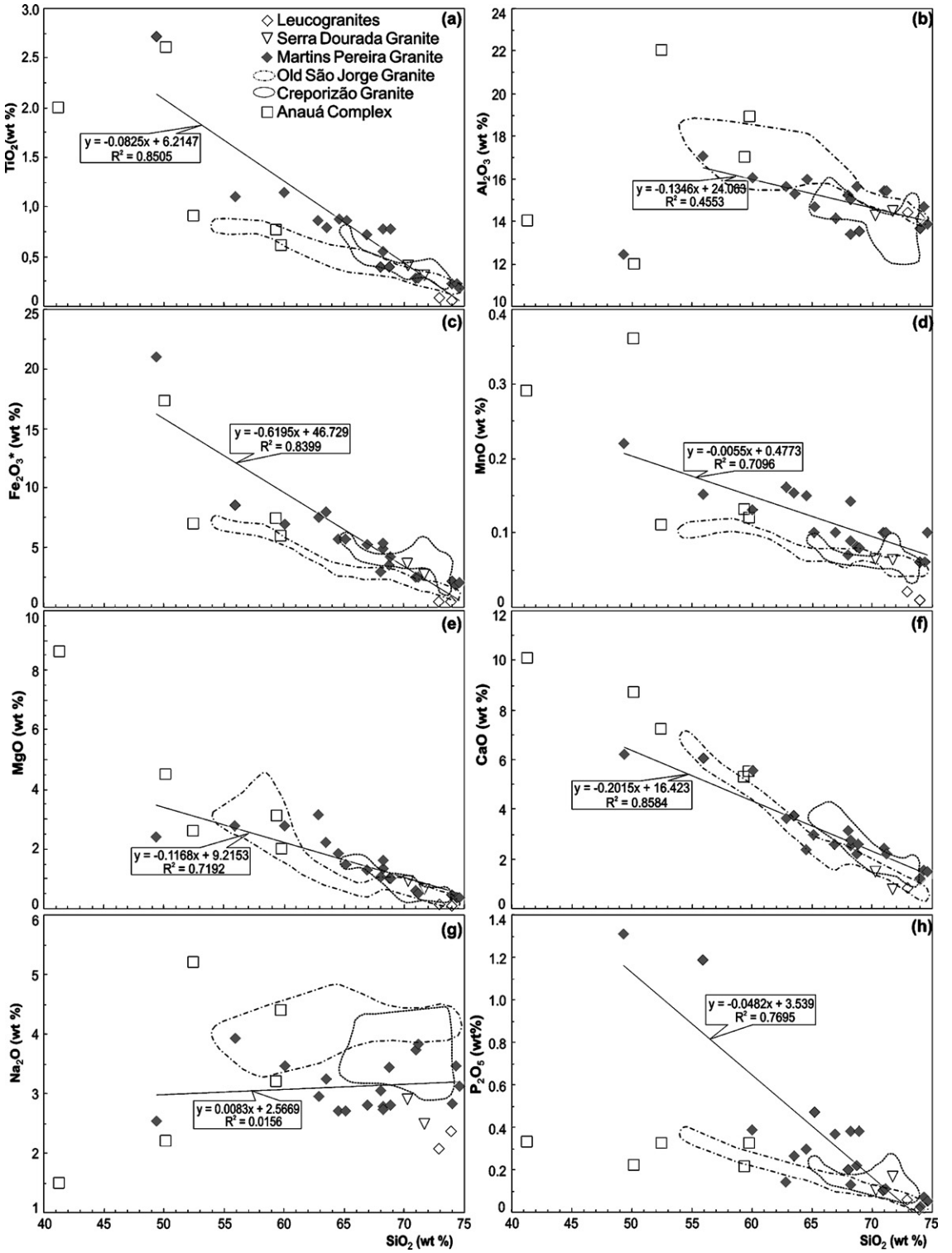

Fig. 3. (a–h) Selected Harker variation diagrams for Martins Pereira and Serra Dourada Granites, leucogranites and Anauá Complex. For references see Table 1. Fields representing Creporizão (CPRM, 2000b) and Old São Jorge granites (Lamarão et al., 2002) of the Tapajós Domain are plotted for comparison. For the linear regression are used only the Martins Pereira Granite samples.

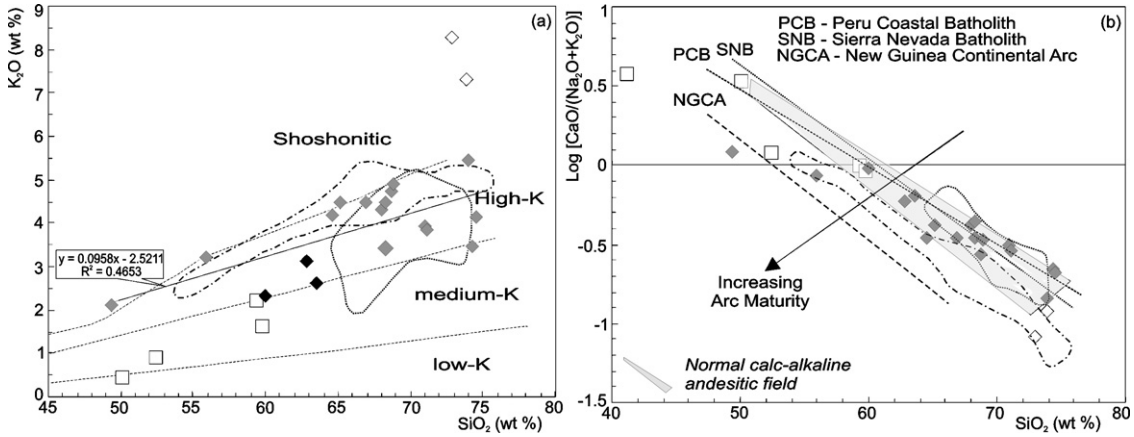

Fig. 4. Geochemical diagrams showing results from Martins Pereira Granite, leucogranites and Anauá Complex rocks (for references see Table 1). Fields representing Creporizão (CPRM, 2000b) and Old São Jorge granites (Lamarão et al., 2002) are plotted for comparison: (a) K_2O *vs.* SiO_2 contents displaying the shoshonite, high-K, medium-K and low-K fields (from Peccerillo and Taylor, 1976; modified by Rickwood, 1989). For the linear regression are used only the Martins Pereira Granite samples. (b) log[CaO/($Na_2O + K_2O$)] *vs.* SiO_2 contents (from Brown et al., 1984). Symbols as in Fig. 3.

instance, leucogranites with the same SiO_2 contents as Martins Pereira granatoid rocks, have low Na_2O (Fig. 3g), MnO (Fig. 3d), $Fe_2O_3 + FeO$ (Fig. 3c) and very high K_2O (Fig. 4a) values.

Rock samples from Martins Pereira Granite are also characterized by linear trends in the all Harker diagrams (Fig. 3a–h). In these diagrams, excluding Na_2O *versus* SiO_2, the statistic parameters show negative linear correlations with regression agreement between 99% and 99.9%. Linear trends can result from several petrogenetic processes, such as contamination, mixing, crystal fractionation with no crystallizing phases change and partial melting (*e.g.* Cox et al., 1987; Wilson, 1991). The lack of significant compositional gaps in Harker diagrams for Martins Pereira samples suggests that the main petrogenetic process is likely related to partial melting or crystal fractionation with no change in the mineral assemblage being fractionated. However this last one requires a great volume of mafic parental magma, not detected in the region. The same is true for fractional crystallization process with change in the crystallizing mineral phases (e.g. hornblende out and biotite in), but in this case the result are usually results in curvelinear Harker-plot trends (*e.g.* Cox et al., 1987; Wilson, 1991) that are not observed for Martins Pereira samples.

In contrast to the Martins Pereira samples, the Anauá Complex and related rocks show lower SiO_2 contents ranging from 41.3% to 59.8% (Table 1), and dispersion in the Harker diagrams (*e.g.* TiO_2, MnO, Al_2O_3, Na_2O and Fe_2O_{3t}). When compared to the Martins Pereira granitoid rocks, the Anauá samples are characterized by lower K_2O and P_2O_5 contents (Figs. 4a and 3h) while having higher Na_2O and MgO (Fig. 3e–g) contents. The Serra Dourada Granite shows remarkable low Na_2O (Fig. 3g) and K_2O contents (Table 1).

Compared to the Martins Pereira granitoid rocks, the 1.99–1.96 Ga Old São Jorge and Creporizão granites from the Tapajós Domain have lower TiO_2 (Fig. 3a), MnO (Fig. 3d) and P_2O_5 (Fig. 3h), and higher Na_2O (Fig. 3g) contents. The corresponding Harker diagrams demonstrate that the Creporizão granites have a shorter range and higher contents of SiO_2 (65.2–73.4%, Table 1), as well as lower MnO (Fig. 3d), Al_2O_3 (Fig. 3b) and K_2O (Fig. 4a) contents.

In the log[CaO/($Na_2O + K_2O$)] *versus* SiO_2 diagram (Fig. 4b), all the studied granitoid rocks (excluding Serra Dourada Granite) indicate calc-alkaline affinity, with the samples plotting in the normal calc-alkaline andesitic field. Only the Old São Jorge Granite shows exclusive transitional character between normal and mature arc series. Most of the granitoid samples also plot in the high-K field (K_2O *versus* SiO_2 diagram, Fig. 4a), however, the Martins Pereira and Old São Jorge granites have a transitional high-K to slightly shoshonitic character. It is also apparent from the K_2O *versus* SiO_2 diagram that samples from the Creporizão Granite display a transitional high-K to locally medium-K trend, whereas Anauá types are medium-K to slightly low-K. The leucogranites show high K contents (>7%) and a highly fractionated character.

The Martins Pereira and Creporizão granite compositions are transitional between metaluminous to peraluminous, while the Old São Jorge granite is metaluminous to slightly peraluminous (Fig. 5a). Almost

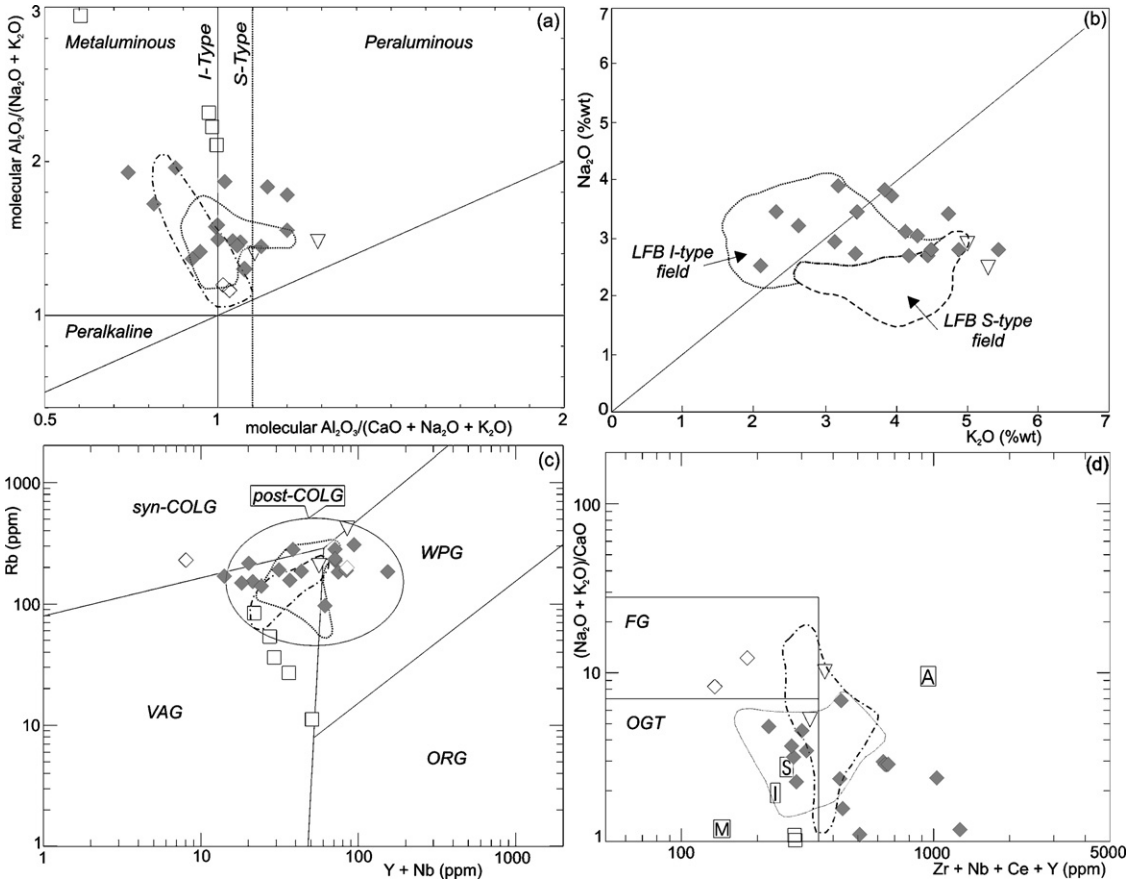

Fig. 5. Martins Pereira and Serra Dourada granites, leucogranites and Anauá Complex samples plotted in the diagrams (for references see Table 1): (a) Molecular $Al_2O_3/(Na_2O + K_2O)$ *vs.* molecular $Al_2O_3/(CaO + Na_2O + K_2O)$ (Maniar and Piccoli, 1989; mod. Shand, 1927) and (b) Na_2O *vs.* K2O plots showing S-type and I-type granites compositional data from Lachlan Folded Belt (LFB); (c) Rb *vs.* (Y + Nb) and (d) $(K_2O + Na_2O)/CaO$ *vs.* (Zr + Nb + Ce + Y). Fields representing Creporizão (CPRM, 2000b) and Old São Jorge granites (Lamarão et al., 2002) are plotted for comparison. (c) VAG, Volcanic Arc Granites; ORG, Ocean Ridge Granites; syn-COLG, syn-collisional Granites; WPG, Within-Plate Granites, fields are from Pearce et al. (1984) and post-COLG (post-collisional granites) from Pearce (1996). (d) OGT, Orogenic granite types: unfractioned I- and S-type granites; FG, Fractionated felsic I- and S-type granites, fields are taken from Whalen et al. (1987). Compositional average of A-, M-, I-, S- and I-type are also represented. Symbols as in Fig. 3.

all these granites show A/NK molar ratios < 2. Only the Anauá Complex rocks (A/NK molar > 2) and the lenses of leucogranite are metaluminous and peraluminous. The Serra Dourada Granite is broadly peraluminous, plotting in the S-type granite compositions. This granite body shows A/CNK molar ratios of 1.1 and 1.3, while some samples of the Martins Pereira Granite also show locally high A/CNK values. In the Na_2O *versus* K_2O diagram, the Martins Pereira granitoid rocks plot on the I-type field, but several samples also plot near to the S-type field boundary (Fig. 5b) showing, as well as the Serra Dourada Granite samples, the lowest Na_2O/K_2O ratios.

In the Rb *versus* (Y + Nb) tectonic discriminator diagrams (Fig. 5c), the Martins Pereira granite samples show transitional VAG (granites to granodiorites) to WPG (biotite-rich tonalites) trends. Anauá rock-types generally plot in the VAG field, with correspondingly low Rb contents. The Creporizão and Old São Jorge granites samples dominantly plot in the VAG field, falling near to the WPG boundary. Thus, excluding Anauá rocks, most of the analyzed samples fall in the postcollisional field of Pearce (1996), which suggests an increasing in arc maturity (Brown et al., 1984; see Fig. 4a) or the beginning of the transition from calc-alkaline to alkaline magmatic series in orogenic to post-orogenic tectonic settings (Bonin, 1990; Barbarin, 1999).

In the $(K_2O + Na_2O)/CaO$ *versus* (Zr + Nb + Ce + Y) diagram (Fig. 5d), the calc-alkaline Martins Pereira, Creporizão and Old São Jorge granites plot on the unfractionated S- and I-type granites to transitional A-type fields. Concerning the Martins Pereira granitoid rocks, the higher Zr, Y and Ce contents are probably related

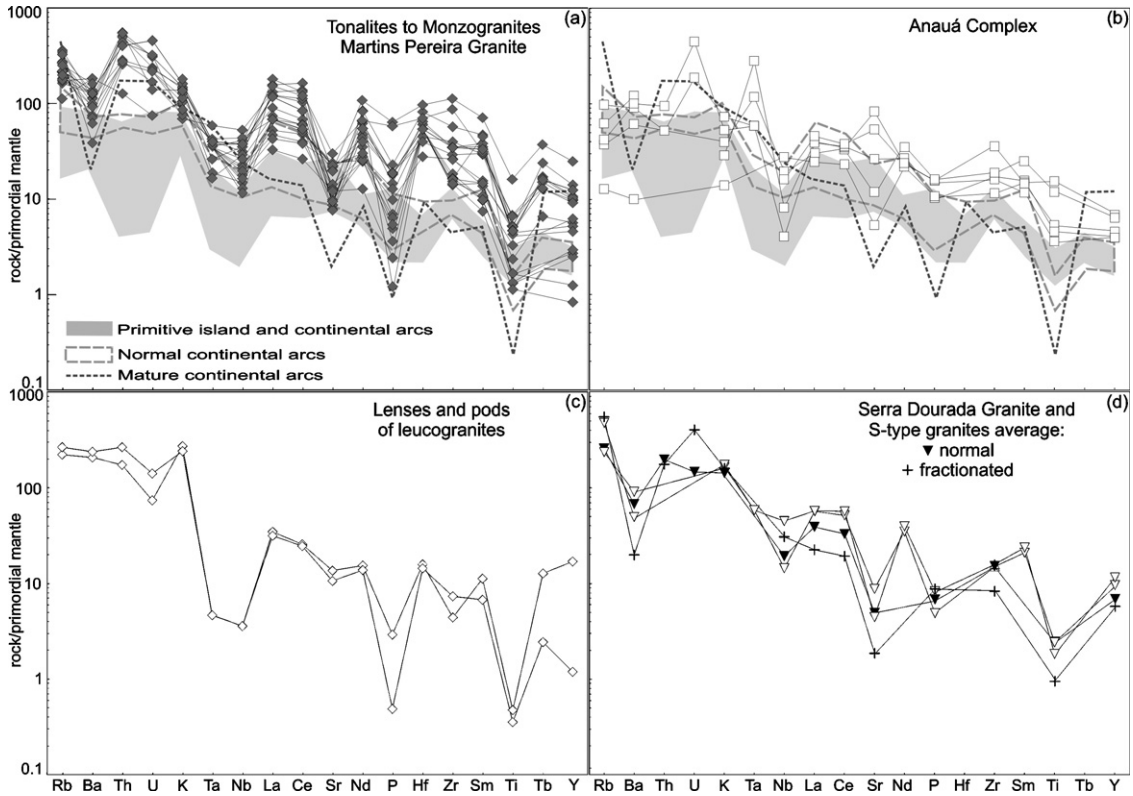

Fig. 6. Primitive mantle-normalized spidergram (Wood, 1979) for (a) Martins Pereira granitoids (tonalites to monzogranites); (b) Anauá Complex; (c) Pods and lenses of leucogranites, and (d) Serra Dourada Granite. Data from granitoids of primitive, normal and mature arcs (Brown et al., 1984) are also plotted for comparison. Symbols as in Fig. 3.

to the presence of accessory minerals such as epidote, allanite and zircon, mainly in biotite-rich tonalite types. However, their metaluminous to peraluminous nature (Fig. 5a) and VAG character (Fig. 5c) point to I-type granite affinity. Samples from Anauá Complex plot in the unfractionated S- and I-type granites field with low $(K_2O + Na_2O)/CaO$ ratios. Only the blobs of leucogranites and few Creporizão Granite samples plot on the fractionated felsic granites field (Fig. 5d).

In the primordial mantle-normalized spidergrams, the Martins Pereira Granite (Fig. 6a) exhibits depleted trace element patterns for some HFSE such as Ta, Nb, P and Ti, and does not show significant LILE depletion (*e.g.* Sr and Ba), as observed for alkali-calcic granitoid rocks of more mature arcs (Brown et al., 1984). This pattern is somewhat similar to those of the calc-alkaline granitoid rocks from normal arcs (cf. Brown et al., 1984), though some samples of the Martins Pereira Granite show strong Ti and P depletion, like the average of mature arc granitoid rocks. This geochemical behavior suggests that Martins Pereira Granite belongs to transitional granitic magmatism, from normal to mature continental arcs (see also Fig. 4a).

The Anauá spidergram pattern (Fig. 6b) displays coherent Rb, Ba and K contents with primitive arcs (Brown et al., 1984), however, U, Ta, Zr, Sm, Ti and Y are enriched in relation to the primitive arc pattern. All other elements (Th, Nb, La, Ce, Sr and P) in the Anauá rocks show primitive to mature arcs transitional values. The spidergram pattern of the blobs and lenses of leucogranite (Fig. 6c) displays the higher Nb, Ta, La, Ce and Hf fractionated values and steeply negative P and Ti anomalies. The leucogranites also show moderate to high Rb, Ba, Th and K contents in relation to chondrite values. The Serra Dourada Granite (Fig. 6d) has Rb, Ba, Sr, P and Ti (locally Rb, Nb and P) pattern remarkably similar to the normal S-type average and La, Ce and Y display more enriched contents than normal S-type granites (*e.g.* Chappell and White, 1992).

4.2. Rare earth element (REE) geochemistry

The total REE contents of the studied granitoid rocks are relatively similar (Table 1), except in the Anauá Complex (138–148 ppm) and leucogranites (100–153 ppm) samples. Martins Pereira (97–624 ppm) and Creporizão

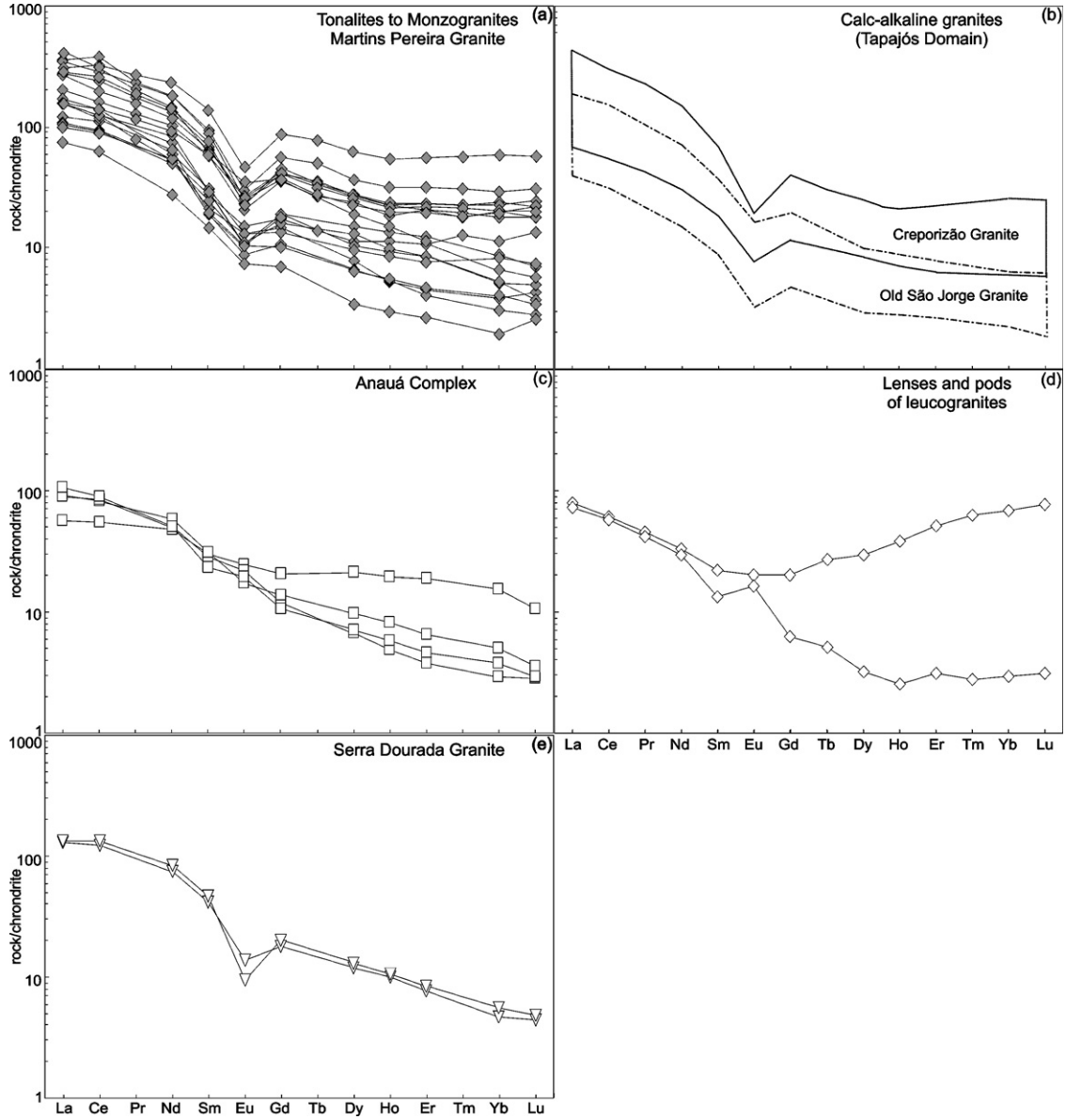

Fig. 7. REE chondrite-normalized diagrams (Boynton, 1984) for (a) Martins Pereira granitoids (tonalites to monzogranites); (b) Creporizão (CPRM, 2000b) and old São Jorge (Lamarão et al., 2002) granites; (c) Anauá Complex; (d) lenses of leucogranites and (d) Serra Dourada Granite. Symbols as in Fig. 3.

granites (104–541 ppm) show some REE enriched samples, contrasting with Old São Jorge Granite which displays moderate to low REE contents (52–244 ppm).

The REE chondrite-normalized pattern of the Martins Pereira Granite (Fig. 7a) is enriched in the LREE (*e.g.* La with 80× to 400× the chondrite values), but the LREE fractionation [$(La/Sm)_n$ ratios range from 3.4 to 6.7, exceptionally 8.0] is similar to the Creporizão and Old São Jorge granites (Fig. 7b). By contrast, the Anauá Complex (Fig. 6c) shows lower LREE contents (*e.g.* La with 50× to 100× the chondrite values) and low $(La/Sm)_n$ ratios (1.9–4.6). The Anauá REE pattern is probably controlled by hornblende and allanite-epidote fractionation.

The Martins Pereira Granite shows variable HREE contents (*e.g.* Yb and Lu ranging 3× to 60× the chondrite values) and the degree of HREE fractionation [$(Gd/Yb)_n$] is similar to the Creporizão, Old São Jorge and Anauá granites (1.1–4.5). In the more HREE enriched granites, the HREE patterns are normally flat. The wide HREE range in the Martins Pereira types is probably associated to the variable residual zircon retention dur-

ing partial melting process and different Zr saturation level of magma (Watson and Harrison, 1983). The same is observed in the leucogranite samples, though these samples have atypical REE patterns, including positive to weakly negative Eu anomaly, which point out for cumulatic plagioclase occurrence (Fig. 7d). These REE patterns may be also related to high hydrothermal activity in the final stages of crystallization or chemical heterogeneities related to source(s). The Old São Jorge (Fig. 7b) and Anauá (Fig. 7c) granitoid rocks exhibit the most HREE depleted patterns.

The Anauá types show discrete negative to positive Eu anomaly, with Eu_n/Eu^* ratios ranging from 0.8 to 1.2 (Table 1; Fig. 7c), suggesting occurrence of cumulate plagioclase and/or hornblende fractionation. Overall, the REE and Eu anomaly patterns (Fig. 7a,b; Table 1) are similar among Martins Pereira ($Eu_n/Eu^* = 0.4–0.7$), Creporizão ($Eu_n/Eu^* = 0.3–0.8$) and Old São Jorge ($Eu_n/Eu^* = 0.4–1.0$) granites. In the case of Martins Pereira, the moderate to discrete negative Eu anomaly probably demonstrates variable residual plagioclase retention in the residue.

The Serra Dourada S-type granite (Table 1; Fig. 7e) shows moderate total REE content (205–223 ppm) and moderate to high negative Eu anomaly ($Eu_n/Eu^* = 0.5–0.3$). The LREE fractionation [$(La/Sm)_n = 3.2–2.8$] and HREE fractionation are moderate to high [$(Gd/Yb)_n = 3.6–3.8$].

5. Martins Pereira and Serra Dourada granites: petrogenetic considerations

The Martins Pereira Granite is one of the most prominent examples of Orosirian high-K calc-alkaline plutonism in southern Roraima, outcropping in the Northern Uatumã-Anauá Domain. The geological literature (*e.g.* Roberts and Clemens, 1993; Barbarin, 1999) shows that the high-K calc-alkaline granitoid rocks are very common in orogenic belts since Proterozoic times, corresponding to 35–40% of all post-Archean metaluminous granitoid rocks found around the world. The two main tectonic environments envisaged for high-K magma generation are (Roberts and Clemens, 1993): (a) continental arc (Cordirellan- or Andean-type), and (b) post-collisional (Caledonian-type) settings.

In general, the tectonic setting discrimination diagrams (*e.g.* Pearce et al., 1984) diagnose the settings in which the protoliths were formed better than the environment where the magma was generated (*e.g.* Barbarin, 1999). This implies that these diagrams could denote geochemical (and isotopic) characteristics of the sources (inheritance), irrespective of the residual mineral components. In the hornblende-free Martins Pereira high-K calc-alkaline granitoid rocks, for instance, linear and continuous trends in Harker diagrams and absence of coeval and large mafic batholiths suggest that the rocks were generated by partial melting processes. However, the sources are not yet fully understood, despite a number of geochemical features (*e.g.* K, U, Th, Rb and REE enrichment) pointing towards the importance of crustal rocks in the magma source.

Experimental data on the potential sources for high-K calc-alkaline granitoid rocks have suggested several possibilities of crustal sources (*e.g.* Roberts and Clemens, 1993). These partial melting hypotheses yield compositional differences among magmas produced by partial melting of common crustal rocks, such as amphibolites, tonalitic gneisses, metagreywackes and metapelites under variable melting conditions (*e.g.* Patiño-Douce, 1996, 1999). This compositional variation can be visualized in terms of major oxides ratios (Fig. 8a–c) or molar oxide ratios (Fig. 8d). It can be seen in these plots that partial melts derived from mafic to intermediate source rocks have lower $Al_2O_3/(FeO + MgO + TiO_2)$, $(Na_2O + K_2O)/(FeO + MgO + TiO_2)$ and molar $Al_2O_3/(MgO + FeO_{tot})$ ratios relative to those originated from metapelites and metagreywackes (Fig. 8a–d).

Most Martins Pereira Granite samples generally plot in the amphibolite and metabasalt–metatonalite fields (Fig. 8a–d), showing low $Al_2O_3/(FeO + MgO + TiO_2)$, $(Na_2O + K_2O)/(FeO + MgO + TiO_2)$ and molar $Al_2O_3/(MgO + FeO_{tot})$ ratios, but exhibit relatively high $CaO/(FeO + MgO + TiO_2)$. This feature, associated with relatively high $Mg^{\#}$ values (32.5–45.3), precludes a derivation from felsic pelite and/or metagreywacke for Martins Pereira Granite, particularly the low-SiO_2 samples (<65%). The SiO_2-rich samples (>65%), however, have lower $Mg^{\#}$ values (24.7–30.7), higher $Al_2O_3/(FeO + MgO + TiO_2)$ and $(Na_2O + K_2O)/(FeO + MgO + TiO_2)$ ratios, and lower $Al_2O_3 + FeO + MgO + TiO_2$ (15–18%) and $Na_2O + K_2O + FeO + MgO + TiO_2$ (8–10%) contents. These Martins Pereira SiO_2-rich samples, as well as the Serra Dourada Granite samples, also show low $CaO + FeO + MgO + TiO_2$ contents (2–4%) and plot in the metagreywacke field (Fig. 8a–d), suggesting metasedimentary source contribution (at least locally) in the Martins Pereira magma genesis. The most suitable metasedimentary source rocks available in the Northern Uatumã-Anauá Domain are related to the Cauarane Group.

By combining the above, mentioned geochemical features with petrographic and other geochemical parameters, the Serra Dourada Granite is considered as

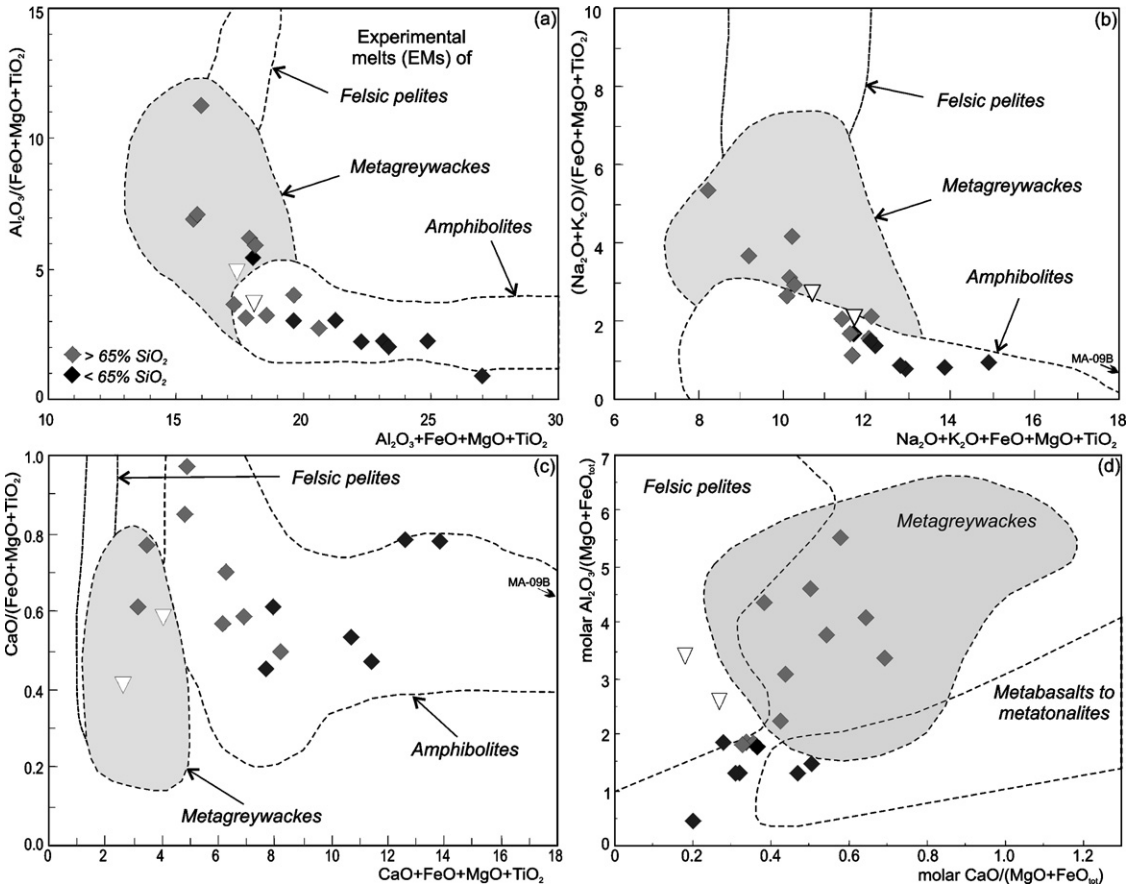

Fig. 8. Martins Pereira and Serra Dourada Granites samples plotted on the (a) $Al_2O_3/(FeO + MgO + TiO_2)$ *vs.* $Al_2O_3 + FeO + MgO + TiO_2$; (b) $(Na_2O + K_2O)/(FeO + MgO + TiO_2)$ *vs.* $Na_2O + K_2O + FeO + MgO + TiO_2$; (c) $CaO/(FeO + MgO + TiO_2)$ *vs.* $CaO + FeO + MgO + TiO_2$; (d) molar $Al_2O_3/(MgO + FeO_{tot})$ *vs.* molar $CaO/(MgO + FeO_{tot})$ diagrams. Outlined fields denote compositions of partial melts obtained in experimental studies by dehydration melting of felsic pelites, metagreywackes, amphibolites–metabasalts and metatonalites sources (Wolf and Wyllie, 1994; Patiño-Douce, 1999; Patiño-Douce and Beard, 1996; Thompson, 1996, and references therein). Symbols as in Fig. 3. See text for discussion.

dominantly derived from a metagreywacke source by a partial melting. In contrast to the Serra Dourada Granite, the Martins Pereira granitic magma could be linked with the partial melting of amphibolite sources, and further input of metagreywacke sources, either by partial melting or contamination–assimilation processes. A similar hybrid origin was proposed by Sardinha (1999) for the 1.89 Ga Igarapé Azul Granite (Almeida et al., 2002). Similarly, an origin for high-K, calc-alkaline I-type granitoid rocks by partial melting of metagreywacke-sources was also proposed by Barker et al. (1992), Altherr et al. (2000) and Thuy Nguyen et al. (2004), in Alaska, Germany and Vietnam, respectively.

6. Zircon geochronology

Five fresh granitic rocks of Northern Uatumã-Anauá Domain were sampled and analyzed by Pb-evaporation and U–Pb ID-TIMS methods (Table 2). Three samples from Martins Pereira Granite and one form leucogranite lenses were analyzed by zircon Pb-evaporation, whereas the same sample from Serra Dourada Granite was analyzed by both methods.

6.1. Martins Pereira Granite (MA-172A, 061A and 007A samples)

In the general sense, hornblende-free Martins Pereira (meta)granitoid rocks are composed of porphyritic coarse- to medium-grained granodiorites, monzogranites and rare fine- to medium-grained (epidote)-biotite-rich tonalites (calc-alkaline granodioritic trend in QAP diagram), locally associated with very small lenses and blobs of leucogranites. Three samples from the Martins Pereira Granite were analyzed by the single-zircon Pb evaporation method (Table 2): cataclastic porphyritic

Table 2
Petrography summary and geographic coordinates of analyzed samples by the single-zircon Pb-evaporation and U–Pb ID-TIMS methods

Sample code	Stratigraphic unit	Geog coord N	Geog coord W	Sample description	U–Pb ID TIMS	MSWD	Pb-evap	USD
MA-172A	Martins Pereira Granite	01°02′49″N	59°55′51″W	Biotite porphyritic monzogranite with abundant tabular and ovoid alkalifeldspar megacrystals. The matrix is isotropic, coarse grained with local cataclastic texture.	–	–	1975 ± 6 (6)	2.9
MA-061A	Martins Pereira Granite	01°01′43″N	60°01′29″W	Biotite mylonitic granodiorite, fine- to medium grained matrix with protomylonitic to mylonitic textures and NE-SW foliation (granolepidoblstic). Titanite and epidote are the main accessory minerals.	–	–	1973 ± 2 (8)	1.4
MA-007A	Martins Pereira Granite	00°59′39″N	60°24′21″W	Biotite porphyritic metamonzogranite, medium to coarse grained matrix and accessory minerals such as epidote, magnetite and minor apatite, titanite, allanite and zircon. ENE-WSW foliation locally filled by subconcordant blobs and lenses of leucogranite.	–	–	1971 ± 2 (4)	1.1
MF-156	Serra Dourada Granite	01°18′03″N	54°00′20″W	Equigranular monzogranite coarse to medium-grained showing aluminous minerals such as biotite, muscovite and locally cordierite (pinitized) and sillimanite. Dynamic recrystallization and planar fabrics are subordinated.	Upper 1962 ± 6	1.7	1948 ± 11 (2)	2.0
					Lower 156 ± 30	–	2138 ± 3 (2)	0.1
MA-246C2	Blobs and lenses of leucogranites	01°11′11″N	60°17′38″W	White grayish, equigranular, leucogranite in lenses and pods with isotropic fabrics, locally showing dynamic recrystalization and cataclasis. The mineral assemblage is composed by alkalifedspar, quartz, plagioclase, biotite, muscovite, epidote, and rare opaque minerals, allanite, titanite, apatite and zircon.	–	–	2354 ± 6 (1)	2.2
					–	–	2134 ± 15 (3)	5.3
					–	–	1997 ± 8 (2)	0.1
					–	–	1959 ± 5 (4)	2.1
					–	–	1909 ± 6 (5)	4.1

Notes: In parenthesis the number of zircon analyses used to calculate the age. *Key*: U–Pb ID TIMS. Conventional U–Pb results, Pb-evap, Pb-evaporation results.

Table 3
Zircon single-crystal Pb-evaporation isotopic data from Martins Pereira Granite (MA-172A, 061A and 007A), Serra Dourada Granite (MF-156) and lense of leucogranite (MA-246C2) samples

Sample/zircon number	Temperature (°C)	Ratios	$^{204}Pb/^{206}Pb$	2σ	$^{208}Pb/^{206}Pb$	2σ	$^{207}Pb/^{206}Pb$	2σ	$(^{207}Pb/^{206}Pb)c$	2σ	Age	2σ	Th/U
Martins Pereira Granite—porphyritic (ovoids) biotite monzogranite													
MA-172A/1	1550	8/8	0.000110	14	0.17363	181	0.12186	15	0.12186	15	1984	2	0.49
MA-172A/2	1500	34/34	0.000019	2	0.12364	21	0.12141	26	0.12119	29	1974	4	0.35
MA-172A/3	1450	30/38	0.000402	3	0.12353	30	0.12674	60	0.12094	40	1971	6	0.35
MA-172A/4	1450	20/20	0.000155	16	0.11822	39	0.12336	39	0.12089	20	1970	3	0.33
	1500	34/34	0.000068	5	0.15392	19	0.12260	15	0.12169	12	1981	2	0.44
MA-172A/5	1500	36/36	0.000120	2	0.12514	28	0.12290	14	0.12131	14	1976	2	0.35
	1550	16/16	0.000000	0	0.11807	95	0.12070	19	0.12070	19	1967	3	0.33
MA-172A/6	1500	30/30	0.000116		0.17099	111	0.12372	16	0.12216	21	1988	3	0.48
		208 (216)			USD: 2.9					Mean age	1975	6	
Martins Pereira Granite—mylonitic biotite monzogranite													
MA-061A/02	1550	40/40	0.000251	3	0.10772	23	0.12506	17	0.12117	36	1974	11	0.30
MA-061A/03	1450	8/8	0.000000	1	0.09694	97	0.12028	73	0.12028	73	1961	22	0.27
MA-061A/04	*1450#*	*0/24*	*0.000456*	*44*	*0.10745*	*26*	*0.12590*	*11*	*0.12590*	*11*	*2042*	*2*	*0.30*
	*1500**	*0/6*	*0.000000*	*1*	*0.10825*	*112*	*0.12591*	*72*	*0.12590*	*72*	*2042*	*10*	*0.31*
MA-061A/05	*1450#*	*0/30*	*0.000647*	*15*	*0.22820*	*963*	*0.12116*	*23*	*0.12116*	*23*	*1848*	*21*	*0.65*
MA-061A/06	1450	8/8	0.000052	6	0.16154	101	0.12162	15	0.12162	15	1970	6	0.46
MA-061A/07	1450	32/32	0.000085	3	0.14130	56	0.12211	15	0.12119	9	1974	3	0.40
MA-061A/09	1450	26/26	0.000267	8	0.11054	20	0.12485	17	0.12123	25	1975	7	0.31
	*1500**	*0/8*	*0.000115*	*4*	*0.13236*	*32*	*0.12406*	*26*	*0.12253*	*27*	*1994*	*4*	*0.37*
MA-061A/10	1450	28/28	0.000191	5	0.13814	32	0.12331	26	0.12117	33	1978	5	0.39
MA-061A/11	*1450**	*0/28*	*0.000168*	*6*	*0.11267*	*89*	*0.12126*	*31*	*0.12126*	*31*	*1941*	*9*	*0.32*
MA-061A/12	1450	8/8	0.000361	26	0.21707	24	0.12526	15	0.12526	15	1963	11	0.61
	1500	8/8	0.000075	1	0.19636	48	0.12124	43	0.12124	43	1960	13	0.56
MA-061A/13	1450	36/36	0.000129	1	0.16711	105	0.12264	14	0.12088	15	1969	5	0.47
	1500	40/40	0.000121	2	0.23122	489	0.12259	10	0.12109	12	1973	3	0.67
	1550	30/30	0.000170	13	0.15605	181	0.12312	21	0.12094	13	1970	4	0.44
		264 (360)			USD: 2.9					Mean age	1973	2	
Martins Pereira Granite—porphyritic biotite metamonzogranite													
MA-007A/01	1540	38/38	0.000071	5	0.14894	18	0.12198	34	0.12107	34	1972	5	0.42
	1550	36/36	0.000082	10	0.15636	141	0.12195	66	0.12074	57	1967	8	0.43
MA-007A/02	*1450**	*0/34*	*0.000102*	*27*	*0.16074*	*447*	*0.12040*	*54*	*0.11883*	*89*	*1939*	*13*	*0.46*
MA-007A/04	1500	36/36	0.000081	4	0.24268	34	0.12158	43	0.12076	30	1968	4	0.69

Table 3 (*Continued*)

Sample/zircon number	Temperature (°C)	Ratios	$^{204}Pb/^{206}Pb$	2σ	$^{208}Pb/^{206}Pb$	2σ	$^{207}Pb/^{206}Pb$	2σ	$(^{207}Pb/^{206}Pb)c$	2σ	Age	2σ	Th/U
MA-007A/05	*1450**	*0/28*	*0.000098*	*13*	*0.13021*	*20*	*0.11918*	*27*	*0.11773*	*32*	*1922*	*5*	*0.37*
	1500	32/32	0.000045	7	0.16279	18	0.12159	39	0.12099	48	1971	7	0.46
MA-007A/06	1500	38/38	0.000030	6	0.14321	283	0.12146	22	0.12110	22	1973	3	0.41
		180 (242)			USD: 0.1					Mean age	1971	2	
Serra Dourada Granite—muscovite-biotite monzogranite with cordierite and sillimanite													
MF156/12	1450	26/34	0.000000	0	0.12405	18	0.13301	23	0.13301	23	2138	3	0.35
MF156/15	1450	36/36	0.000037	2	0.08816	21	0.13360	13	0.13299	11	2138	1	0.25
		62 (70)			USD: 0.1					Mean age	2138	3	
MF156/06	1550	4/8	0.000078	7	0.47918	1656	0.12012	17	0.11907	19	1943	3	0.14
MF156/11	1550	6/6	0.000073	28	0.54277	132	0.12102	24	0.12004	44	1957	7	0.15
		10 (14)			USD: 2.0					Mean age	1948	11	
Pods and lenses—leucogranite													
MA-246C2/01	1500	24/24	0.000038	2	0.04358	104	0.15111	46	0.15066	52	2354	6	0.12
	*1550**	*0/8*	*0.000044*	*2*	*0.04139*	*58*	*0.14857*	*78*	*0.14800*	*78*	*2323*	*9*	*0.11*
		24 (32)			USD: 2.2				Mean age (Group I)		2354	6	
MA-246C2/10	1500	36/36	0.000233	13	0.06005	30	0.13863	40	0.13533	56	2169	7	0.17
	1550	8/8	0.000246	106	0.05694	47	0.13545	143	0.13254	47	2132	6	0.16
MA-246C2/14	1450	8/8	0.000423	26	0.10097	44	0.13804	694	0.13248	699	2131	92	0.28
MA-246C2/16	1500	38/38	0.000464	12	0.06177	32	0.13868	42	0.13209	31	2126	4	0.17
	1550	24/32	0.000515	28	0.06177	26	0.13899	29	0.13207	60	2126	8	0.17
		114 (122)			USD: 5.3				Mean age (Group II)		2134	15	
MA-246C2/17	1500	20/20	0.000116	102	0.05330	396	0.12487	87	0.12280	93	1998	13	0.15
MA-246C2/21	1500	34/34	0.000119	28	0.03507	14	0.12453	31	0.12273	68	1997	10	0.10
	*1550**	*0/6*	*0.000000*	*0*	*0.03531*	*29*	*0.12630*	*148*	*0.12630*	*148*	*2047*	*21*	*0.10*
		54 (60)			USD: 0.1				Mean age (Group III)		1997	8	
MA-246C2/07	1500	20/20	0.000270	15	0.05075	55	0.12369	53	0.12004	56	1957	8	0.14
MA-246C2/09	1500	22/22	0.000236	9	0.10952	280	0.12285	87	0.11972	57	1952	9	0.31
MA-246C2/13	1450	8/8	0.000099	4	0.04017	313	0.12051	117	0.11918	118	1944	18	0.11
MA-246C2/23	*1450**	*0/14*	*0.000551*	*22*	*0.04188*	*34*	*0.12441*	*74*	*0.11713*	*57*	*1913*	*9*	*0.12*
	1500	34/34	0.000408	4	0.11232	105	0.12535	27	0.12009	21	1958	3	0.32
	1550	6/6	0.000392	18	0.10542	57	0.12604	30	0.12080	39	1968	6	0.30
		90 (104)			USD: 2.1				Mean age (Group IV)		1959	5	

MA-246C2/05	1500	36/36	0.000340	28	0.06289	153	0.12044	21	0.11578	29	1892	4	0.18
	1550	36/36	0.000111	45	0.04114	280	0.11986	30	0.11842	49	1933	7	0.12
	1580	8/8	0.000430	20	0.06177	158	0.12252	67	0.11674	72	1907	11	0.18
MA-246C2/06	*1450*#	*0/16*	*0.001815*	*73*	*0.09369*	*108*	*0.13676*	*209*	*0.10994*	*108*	*1799*	*18*	*0.27*
	1500	38/38	0.000413	39	0.06081	62	0.12311	27	0.11721	45	1914	7	0.17
	1550	36/36	0.000398	17	0.07336	570	0.12357	31	0.11822	33	1930	5	0.21
	1580	32/32	0.000455	8	0.06004	19	0.12307	41	0.11703	50	1912	8	0.17
MA-246C2/08	1450	8/8	0.000579	40	0.04980	93	0.12373	66	0.11594	86	1895	13	0.14
	1480	30/30	0.000147	4	0.05632	54	0.11870	22	0.11668	16	1906	3	0.17
	1500	38/38	0.000164	11	0.06134	160	0.11910	24	0.11694	19	1910	3	0.19
	1550	12/12	0.000179	2	0.05614	162	0.11889	100	0.11623	61	1899	9	0.17
MA-246C2/18	*1450*#	*0/8*	*0.001175*	*176*	*0.07656*	*957*	*0.12798*	*513*	*0.11209*	*576*	*1834*	*93*	*0.24*
	1500	16/16	0.000368	148	0.05822	30	0.12204	143	0.11686	75	1909	12	0.18
MA-246C2/19	1500	8/8	0.000590	574	0.19248	833	0.12400	688	0.11607	1043	1897	162	0.60
		262 (286)				USD: 4.1			Mean age (Group V)		1909	6	

Notes: Crystal numbers are indicated. The column number of ratios shows the total of isotopic ratios used to the age calculation and, in parenthesis, the total isotopic ratios measured. Evaporation steps in italics were not included in the age calculation of each grain due to: (*) too much higher or lower values of the $^{207}Pb/^{206}Pb$ ratio in relation to the average of the zircon, and (#) $^{204}Pb/^{206}Pb > 0.0004$ (and $^{204}Pb/^{206}Pb > 0.0006$ for the leucogranite sample). Th/U ratios calculation: $Th = [(^{208}Pb/^{206}Pb)/((Th \times T) - 1] + (^{208}Pb/^{206}Pb)$; $U = [(^{208}Pb/^{206}Pb)/((U \times T) - 1] + (^{208}Pb/^{206}Pb)$; $Th = 4.94750 \times 10^{-12}$; $U = 1.55125 \times 10^{-11}$ (in Klötzli, 1999).

monzogranite (MA-172A), mylonitic granodiorite (MA-61A) and porphyritic metamonzogranite (MA-007A).

The sample of cataclastic coarse-grained monzogranite (MA-172A) shows translucent crystals with local opaque portions, pale brown to pale yellow colours, prismatic (length/width ratios between 2.9:1 and 1.8:1) and 90–400 μm in length, exhibiting well-defined faces and vertices. Mineral inclusions (such as apatite and Fe–Ti oxides) and fractures are common. A total of 6 crystals were analyzed yielding a mean age of 1975 ± 6 Ma age (USD: 2.9) from 162 isotopic ratios (Table 3; Fig. 9a). Individual ages of these analyses vary from 1988 to 1962 Ma.

The MA-61A mylonitic biotite granodiorite was sampled along an ENE-WSW mylonitic zone to the north of São Luiz do Anauá town. Two different zircon populations were described in this sample: (a) prismatic (length/width ratios between 2.4:1 and 1.6:1), translucent and brown to pale brown crystals showing fractures and rounded vertices; (b) prismatic (length/width ratios between 3.8:1 and 2:1), transparent, pale yellow crystals showing few fractures and vertices, and well-defined faces. Both zircon populations showed scarce mineral inclusions, crystals with 140–360 μm in length and local irregular internal zoning, this last observation suggesting igneous overgrowth and/or older inherited cores. The mean age of analyses of 8 crystals (264 isotopic ratios) from both populations by the Pb-evaporation method yielded 1973 ± 2 Ma (USD: 2.1) (Table 3; Fig. 9b), exhibiting individual ages varying of 1978–1962 Ma. Anomalous ages were observed in crystals #4 (2042 ± 20 Ma, 1450 and 1500 °C step-heatings) and #9 (1994 ± 4 Ma, 1500 °C step-heating), which could represent inherited components.

The sample of the porphyritic metamonzogranite facies (MA-007A) selected for dating is locally foliated and banded. The zircon crystals are pale brown, transparent to translucent, prismatic and bypiramidal, with 190–450 μm in length (3.5:1 to 2.2:1 length/width ratios). They show fractures, sometimes radial-like, well-defined faces and rounded vertices. Inclusions are very rare in these zircon samples. A total of four crystals were analyzed yielding individual ages varying from 1973 Ma to 1967 Ma, and a mean age of 1971 ± 2 Ma age (Table 3; Fig. 9c). The 25 blocks and 180 isotopic ratios show a very homogeneous pattern, yielding a well-defined mean age with good statistical level (USD: 1.1).

The results obtained from Martins Pereira Granite show a small interval age (1980–1968 Ma) and local 1.99 and 2.04 Ga inheritances, these last probably related to the Anauá Complex. Other granitoid rocks from Martins Pereira Granite area, and equivocally related to

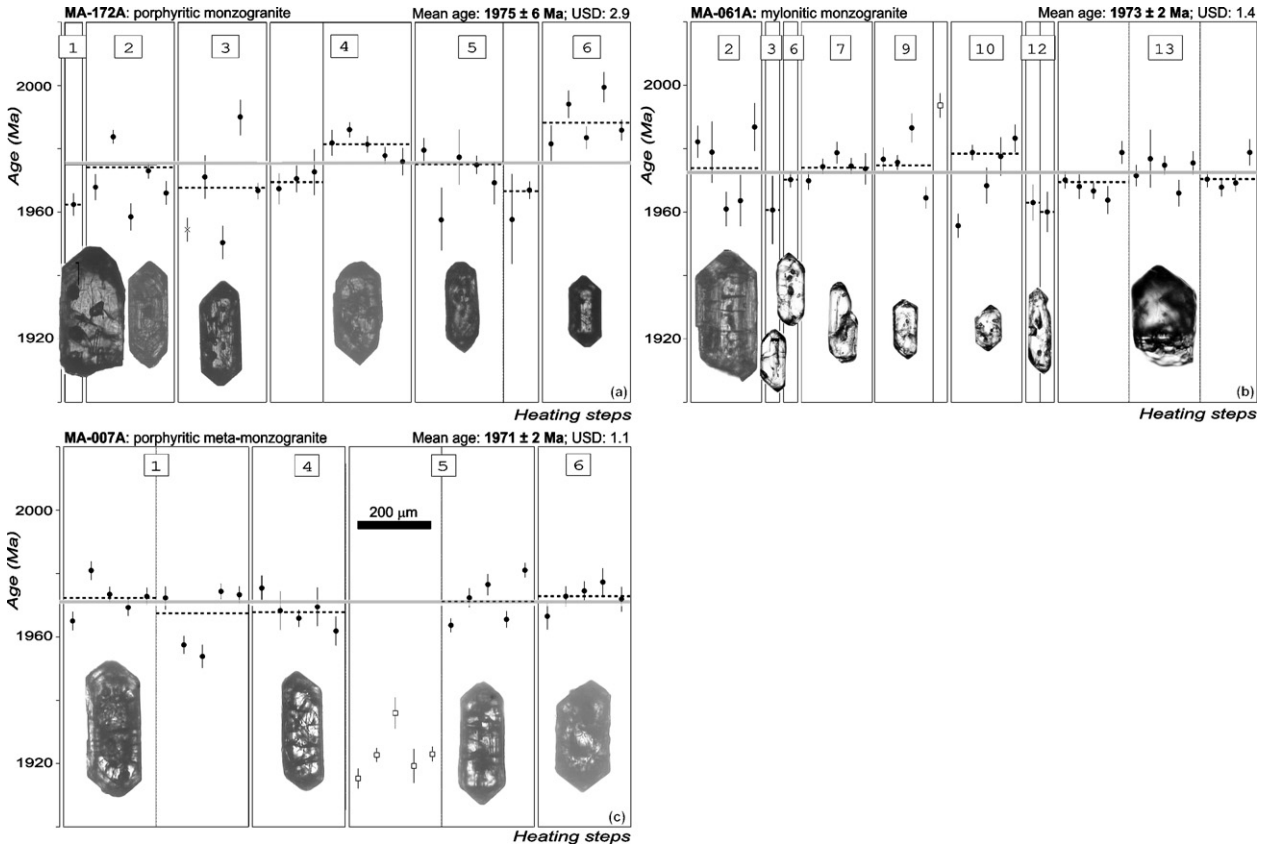

Fig. 9. Single-zircon Pb-evaporation ages for Martins Pereira Granite samples: (a) MA-172A (cataclastic porphyritic monzogranite), (b) MA-061A (mylonitic granodiorite) and (c) MA-007A (foliated porphyritic metamonzogranite). Symbols: filled circle—accepted blocks for age calculation; square—blocks not used due to their higher or lower values of the $^{207}Pb/^{206}Pb$ ratio in relation to the mean; ×—rejected blocks due to show $^{204}Pb/^{206}Pb > 0.0004$. Crystal numbers are indicated (see Table 3). The scale bar is the same for all diagrams.

Água Branca Suite and Igarapé Azul Granite, were dated by Almeida et al. (1997) and CPRM (2003) yielding 1960 ± 21 and 1972 ± 8 Ma, respectively (Table 5). These ages are in agreement with the results obtained in this paper (see Fig. 9a–c) and mark an important magmatic event in southeastern Roraima, here named as Rorainópolis event. In general sense, these results are uniform, homogeneous and establish a 1.97–1.96 Ga age range, despite the observed heterogeneous textures (*e.g.* igneous, mylonitic and cataclastic), different geographical site sampling, and different applied methodologies (Tables 2 and 5; Fig. 2).

6.2. Serra dourada granite (MF-156 samples)

The S-type granitoid rocks in southeastern Roraima State were initially described by Faria et al. (1999) and incorporated into the Igarapé Azul Granite. However, Almeida et al. (2002) subdivided the Igarapé Azul Granite into three different types: Serra Dourada Granite (true S-type), Martins Pereira Granite (I-type high-K calc-alkaline) and the proper Igarapé Azul Granite (I-type felsic high-K calc-alkaline).

A syenogranite sample of Serra Dourada Granite (MF-156) with biotite, muscovite and cordierite (Table 2), including monazite and xenotime as accessory minerals, was analyzed by single-zircon Pb-evaporation method. This sample shows two zircon populations with different features. The first group is scarce and shows rounded vertices, irregular faces (corrosion?), light yellow colour, 310–500 μm in length (length/width ratios between 2.3:1 and 1.5:1), translucent to transparent opacity, and is generally free of inclusions. The second type of zircon shows crystals with slightly rounded vertices, is light brown to brown, 170–340 μm in length (length/width ratios between 3.1:1 and 1.5:1), transparent and locally with few inclusions and fractures. This second type of zircon is characterized by well-developed {2 1 1} pyramid, similar to zircon crystallized from peraluminous melt (Pupin, 1980).

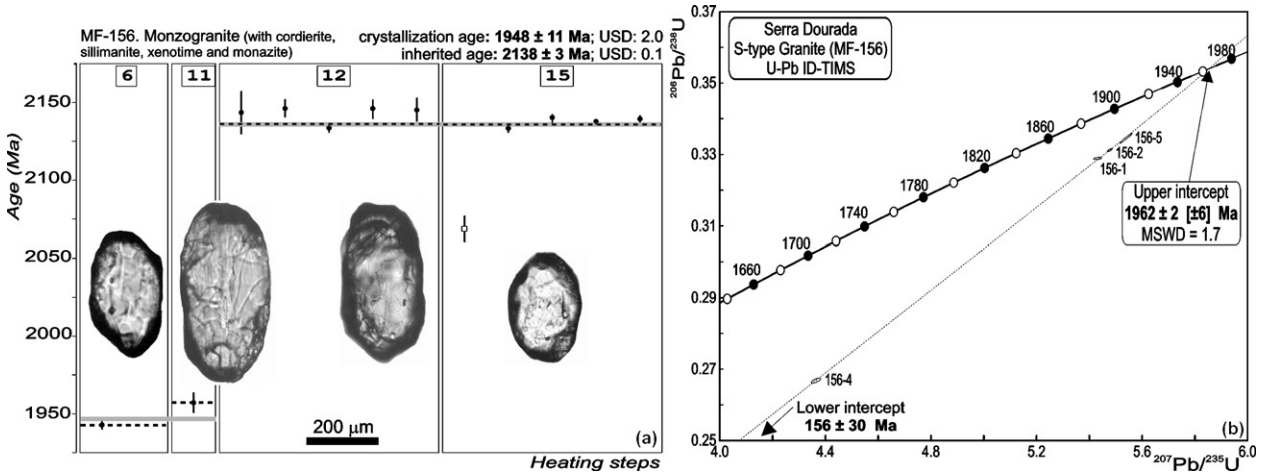

Fig. 10. Single-zircon ages for Serra Dourada Granite (sample MF-156) yielded by (a) Pb-evaporation and (b) U–Pb ID-TIMS (concordia diagram) methods. Crystal numbers are indicated (see Tables 3 and 4). Symbols: filled circle—accepted blocks for age calculation; square—blocks not used due to too low value of the $^{207}Pb/^{206}Pb$ ratio in relation to the average.

In the Pb-evaporation method, the zircon fractions yielded two different age patterns, irrespective of the few analyzed grains and isotopic ratios obtained (Table 3). The lower age (1948 ± 11 Ma) was obtained from two blocks from two crystals. The higher age (2138 ± 3 Ma) was obtained from nine blocks of isotopic ratios from two zircon crystals (Fig. 10a), and is interpreted as an age of inherited origin.

U–Pb ID-TIMS was carried out on the same sample with the aim of interpreting the ages obtained by the Pb-evaporation method. The regression of four experimental points yields a discordia line which indicates an upper intercept at 1962 ± 2 Ma (Table 4; Fig. 10b), interpreted as the crystallization age of the analyzed crystals and, similarly, that of the Serra Dourada Granite. This age is very close to the age yielded with the Pb-evaporation method for the same sample which, taking into account the errors, almost overlap one another.

The geological similarities between Serra Dourada (Uatumã-Anauá Domain) and Taiano (Central Guyana Domain) S-type granites are also pointed out by our U–Pb and Pb-evaporation zircon ages. The Taiano anatetic leucogranite yields 1969 ± 3.5 Ma (zircon U–Pb SHRIMP, CPRM, 2003) and the minimum crystallization age yielded by single-zircon Pb-evaporation (1948 ± 11 Ma) and U–Pb ID-TIMS (1962 + 2/−6 Ma) methods for the Serra Dourada type are quite similar (Table 5), confirming an important anatetic process in the central-southern Roraima State occurred 1.97–1.96 Ga. Other S-type granitoid rocks in the Roraima, such as Curuxuim and Amajari granites (CPRM, 1999), could be related also to this same event, however they are not dated yet.

The inherited ages in both S-type granites also show Eo- to Neo-Transamazonian ages, ranging from 2138 ± 3 Ma (Serra Dourada Granite) to 2047 ± 7 and 2072 ± 3 Ma (Taiano Granite), probably related to sedimentary contribution. This hypothesis is partially confirmed by Transamazonian detrital zircon crystals detected in the metavolcanosedimentary rocks from the Cauarane Group (Table 6), from which two paragneiss samples were dated by U–Pb ID-TIMS (2223 ± 19 Ma, Gaudette et al., 1996) and U–Pb SHRIMP (2038 ± 17 and 2093 ± 62 Ma, CPRM, 2003) methods.

6.3. Leucogranite (MA-246C2 sample)

Leucosyenogranite lens sample (MA-246C2) associated with Martins Pereira (meta)granitoid rocks showed a complex set of results. All zircons were analysed based on 2 sigma = 0.0006, because 2 sigm = 0.0004 yielded ages with higher USD values and errors, although the results are not so different. For instance, the younger zircon population yielded by 2 sigma 0.0006 and 0.0004, 19094 ± 6 Ma (USD = 4.1) and 19094 ± 7 Ma (USD = 4.7), respectively. Five groups of zircon occur in this sample in decreasing age order (Table 5; Fig. 11a and b).

Group I is represented by only one pale brown, transparent to translucent zircon grain with 265 μm in length (length/width ratio 1.9:1), showing regular internal zoning, well-defined faces and dark inclusions in the core. It yielded an age of 2354 ± 6 Ma (crystal #1).

Group II exhibits pale yellow and transparent grains (locally translucent to opaque) being 250-330 μm in length (length/width ratios between 3.2:1 and 2.5:1).

Table 4
U–Pb isotopic zircon data (ID-TIMS) from Serra Dourada granitoid (sample MF-156)

Sample		Concentrations		Atomic ratios							Ages (Ma)			
Zircon number	Weight (mg)	ppm U	ppm Pb	$^{206}Pb/^{04}Pb^{c1}$	%err	$^{207}Pb^{*}/^{235}U^{c2}$	%err	$^{206}Pb^{*}/^{238}U^{c2}$	%err	$^{207}Pb^{*}/^{206}Pb^{*c2}$	%err	$^{206}Pb^{*}/^{238}U$	$^{207}Pb^{*}/^{235}U$	$^{207}Pb^{*}/^{206}Pb^{*}$	Concordant[d] (%)
MF-156-1	0.144	35.20	12.33	129.714	1.040	543.181	0.225	0.328881	0.079	0.119786	0.204	1833	1890	1953	94
MF-156-2	0.304	12.16	4.42	818.679	0.459	547.834	0.152	0.331237	0.118	0.119952	0.088	1844	1897	1956	94
MF-156-4	0.213	18.01	5.29	683.428	0.366	436.517	0.324	0.266823	0.223	0.118652	0.234	1525	1706	1936	79
MF-156-5	0.166	34.19	12.01	233.930	0.793	553.956	0.354	0.334560	0.347	0.120088	0.068	1860	1907	1958	95
MF-156-6	0.770	5.51	1.90	816.957	0.700	536.251	0.457	0.326122	0.394	0.119258	0.231	1820	1879	1945	94

Notes: Maximum total blanks for zircon analyses are 10 pg for Pb and 2 pg for U. Stacey and Kramers (1975) values were used. c1: measure ratios corrected for mass fractionation; c2: ratios corrected for spike, fractionation, blank and initial common Pb following Stacey and Kramers (1975) model. Erros are at 2 s; d: concordance in relation to concordia curve: $100t(^{206}Pb/^{238}U)/t(^{207}Pb/^{206}Pb)$.

Cracks are common, but inclusions are rare. This group comprises three zircon crystals with individual ages varying from 2148 to 2126 Ma, and yielded a mean age of 2134 ± 15 Ma (crystals #10, 14 and 16).

Group III encompasses colorless to pale yellow crystals which are 166–180 μm in length (length/width ratios around 2.7:1), with crystals locally exhibiting internal zoning and cracks in the core. This group yielded 1997 ± 8 Ma as a mean age (crystals #17 and 21).

In general, zircon crystals of the group IV are characterized by brown to pale brown and translucent grains with well-defined faces (locally broken) and 210–260 μm in length (length/width ratios around 2.6:1). This group consists of four crystals with individual ages varying from 1968 to 1952 Ma, and yielded a mean age of 1959 ± 5 Ma (crystals #7, 9, 13 and 23).

Zircon crystals of the group V are 164–330 μm in length (length/width ratios between 3.1:1 and 1.8:1), are pale yellow to pale brown in colour, transparent and show local cracks and inclusions. This group displays a mean age of 1909 ± 6 Ma from five crystals (#5, 6, 8, 18 and 19), with individual ages varying from 1933 to 1892 Ma. This lowest age (group V) is interpreted as the crystallization age, whereas the higher ages (groups I–IV) probably represent inherited zircon of different origins. However, this crystallization age may have, at least locally, grains with igneous border and older cores, suggesting partial contribution of isotopic content of older events (e.g. crystals #5 and 6).

Despite the wide variety of zircon populations from sample MA246C2, including grains with internal complexity or zoning ("mixing age") or partial resetting, the results obtained by the single-zircon Pb-evaporation method allow for the following interpretation:

(a) The 1909 ± 6 Ma (group V) is interpreted as the minimum crystallization age of leucosyenogranite. Other ages, around 1.89–1.90 Ga, which are related to Igarapé Azul and Água Branca granitoids (*e.g.* CPRM, 2003; Almeida et al., 2002) are described in this region, mainly in the southern Uatumã-Anauá Domain. These leucogranitic lenses also show some petrographic similarities with Igarapé Azul granitoid rocks and were both likely generated in the same magmatic event.
(b) The 1997 ± 8 Ma (group III) and 1959 ± 5 Ma (group IV) ages probably correspond to inherited components from the Surumu volcanics and Martins Pereira (meta)granitoid rocks (or Urubu orthogneisses?), respectively, however the former are not exposed in the Uatumã-Anauá Domain and correlated igneous rocks are not found there.

Table 5
Summary of new and previous Pb–Pb and U–Pb (ID-TIMS and SHRIMP) ages yielded by zircon from volcano-plutonic rocks older than 1900 Ma of the Ventuari-Tapajós (or Tapajós-Parima) Province

Symbol	Reference number	Rock type	Lithostratigraphic unit	Age (Ma)	Reference	Method
Central Guyana Domain						
CG1	1	Hornblende-biotite gneiss with titanite (Miracélia Gneiss)	Rio Urubu "A-type" gneisses	1935 ± 5	Fraga (2002)	B
	2	Hornblende-biotite gneiss with allanite (Igarapé Branco Gneiss)	Rio Urubu "A-type" gneisses	1937 ± 5	Fraga (2002)	B
CG2	3	Quartz jotunite	Serra da Prata C-type	1933 ± 2	Fraga et al. (2003)	B
	4	Clinopyroxene porphyrytic charnockite	Serra da Prata C-type	1934 ± 1	Fraga et al. (2003)	B
	5	Hypersthene quartz syenite	Serra da Prata C-type	1934 ± 3	Fraga et al. (2003)	B
	6	Clinopyroxene porphyrytic charnockite	Serra da Prata C-type	1936 ± 4	Fraga et al. (2003)	B
	7	Charnockite hydrothermalized	Serra da Prata C-type	1943 ± 5	Fraga et al. (2003)	B
	8	Quartz jotunite gneiss	Serra da Prata C-type	1966 ± 37	Fraga et al. (1997)	A
CG3	9	Vilhena Mylonite	Rio Urubu "I-type" gneisses	1932 ± 10	CPRM (2003)	D
	10	Mucajaí Metagranite	Rio Urubu "I-type" gneisses	1938 ± 9	CPRM (2003)	D
	11	Granitic gneiss	Rio Urubu "I-type" gneisses	1943 ± 7	Gaudette et al. (1996)	C
	12	Granitic gneiss	Rio Urubu "I-type" gneisses	1944 ± 10	Santos and Olszewski (1988)	C
	13	Tonalite orthogneiss	Rio Urubu "I-type" gneisses	1951 ± 24	Fraga et al. (1997)	A
CG4	14	S-type leucogranite	Taiano S-type	1969 ± 4	CPRM (2003)	D
Surumu Domain						
S1	15	Tabaco Mountain Dacite	Surumu Group	1966 ± 9	Schobbenhaus et al. (1994)	C
	16	Tabaco Mountain Dacite	Surumu Group	1977 ± 8	Schobbenhaus et al. (1994) mod. by CPRM (2003)	C
	17	Uraricáa Rhyodacite	Surumu Group	1984 ± 7	Santos et al. (2003b)	D
	18	Cavalo Mountain Rhyodacite	Surumu Group	2006 ± 4	Costa et al. (2001)	B
S2	19	Orocaima Granodiorite	Pedra Pintada Suite	1956 ± 5	CPRM (2003)	D
	20	Pedra Pintada Monzogranite	Pedra Pintada Suite	2005 ± 45	Almeida et al. (1997)	A
Parima Domain						
P1	21	Prainha meta-andesite	Parima Group	1948 ± 6	Santos et al. (2003c)	D
Uatumã-Anauá Domain						
UA1	22	Leucosyenogranite (ma246c2)	Blobs and lenses of leucogranite	1909 ± 9	This paper	B
UA2	23	Monzogranite (mf156)	S-type Serra Dourada	1948 ± 11	This paper	B
	24	Monzogranite (mf156)	S-type Serra Dourada	1962 ± 6	This paper	C
	25	Metamonzogranite	Martins Pereira Granite	1938 ± 17	Almeida et al. (1997)	A
UA3	26	Metamonzogranite	Martins Pereira Granite	1960 ± 21	Almeida et al. (1997)	A
	27	Metamonzogranite	Martins Pereira Granite	1972 ± 7	CPRM (2003)	C
	28	Metamonzogranite (ma007a)	Martins Pereira Granite	1971 ± 2	This paper	B
	29	Mylonitic monzogranite (ma061a)	Martins Pereira Granite	1973 ± 2	This paper	B
	30	Monzogranite (ma172a)	Martins Pereira Granite	1975 ± 6	This paper	B
UA4	31	Metatonalite	Anauá Complex	2028 ± 9	Faria et al. (2002)	D

Table 5 (*Continued*)

Symbol	Reference number	Rock type	Lithostratigraphic unit	Age (Ma)	Reference	Method
Tapajós Domain						
T1	32	Granite	Creporizão Suite	1957 ± 6	Santos et al. (2000)	C
	33	Creporizão Monzogranite	Creporizão Suite	1963 ± 6	Santos et al. (2001)	D
	34	JL Monzogranite	Creporizão Suite	1966 ± 5	Santos et al. (2001)	D
	35	Joel Monzogranite	Creporizão Suite	1968 ± 7	Santos et al. (2004)	D
	36	km130 Monzogranite	Creporizão Suite	1968 ± 16	CPRM (2000b)	B
	37	Ouro Roxo Metandesite II	Creporizão Suite	1974 ± 6	Santos et al. (2001)	D
T2	38	Biotite leucomonzogranite	Old São Jorge Granite	1981 ± 2	Lamarão et al. (2002)	B
	39	Hornblende-biotite monzogranite	Old São Jorge Granite	1983 ± 8	Lamarão et al. (2002)	B
	40	Granite	Old São Jorge Granite	1984 ± 1	CPRM (2000b)	B
T3	41	Trachyte	Vila Riozinho Volcanics	1998 ± 3	Lamarão et al. (2002)	B
	42	Trachyte	Vila Riozinho Volcanics	2000 ± 4	Lamarão et al. (2002)	B
T4	43	Rio Claro Monzogranite	–	1997 ± 3	CPRM (2000b)	B
	44	Jamanxim Rapakivi Monzogranite	–	1997 ± 5	Santos et al. (1997)	C
T5	45	Cabruá Tonalite	Cuiú-Cuiú Complex	2005 ± 7	Santos et al. (2001)	D
	46	Conceição Tonalite	Cuiú-Cuiú Complex	2006 ± 3	Santos et al. (1997, 2004)	C
	47	Ouro Roxo Andesite	Cuiú-Cuiú Complex	2012 ± 8	Santos et al. (2001)	D
	48	JL Tonalite	Cuiú-Cuiú Complex	2015 ± 9	Santos et al. (2001)	D
	49	Amana Monzogranite	Cuiú-Cuiú Complex	2020 ± 12	Santos et al. (2001)	D
	50	Cuiú-Cuiú Meta-tonalite	Cuiú-Cuiú Complex	2033 ± 7	Santos et al. (2001)	D

Notes: (A) Pb-evaporation on single filament; (B) Pb-evaporation on double filament; (C) U–Pb ID-TIMS; (D) U–Pb SHRIMP. Reference number 1–50 and symbols GC1-T5 are the same as in Fig. 12.

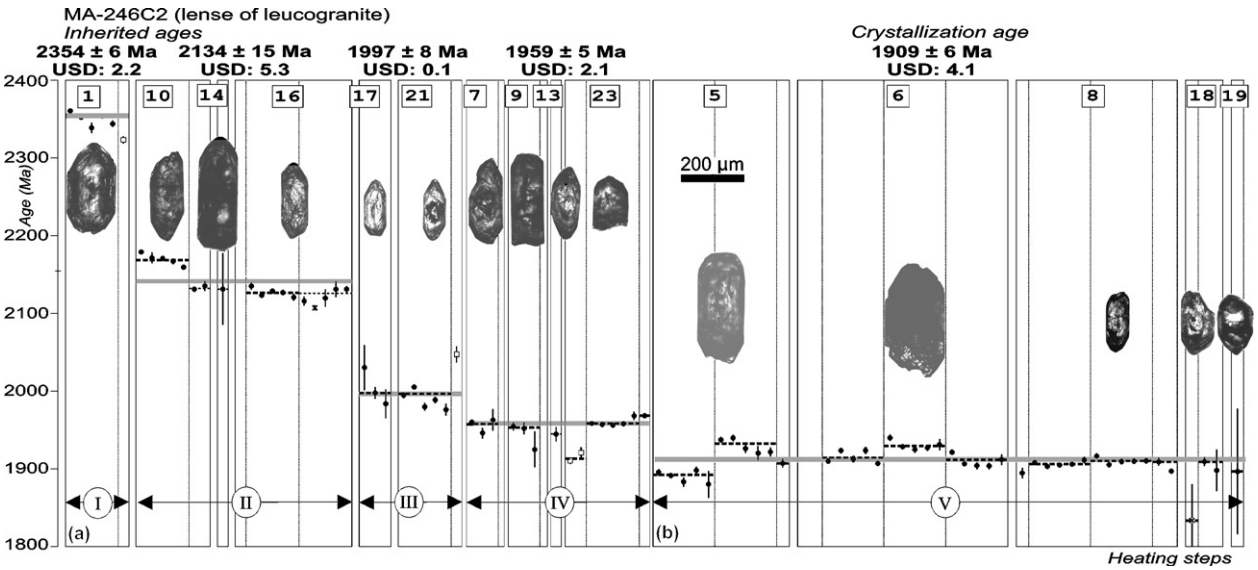

Fig. 11. Single-zircon Pb-evaporation ages of lenses of leucogranite in association with Martins Pereira Granite. (a) Inherited ages: (I) pre-Transamazonian (Siderian); (II) Transamazonian; (III) Late-Transamazonian (Anauá Complex?); (IV) Martins Pereira, and (b) (V) minimum crystallization age. Symbols: filled circle—accepted blocks for age calculation; square—blocks discarded due their higher or lower values of the $^{207}Pb/^{206}Pb$ ratio in relation to the mean; ×—rejected blocks due to $^{204}Pb/^{206}Pb > 0.0006$. Crystal numbers are indicated (see Table 3). The scale bar is the same for all diagrams.

Table 6
Summary of ages and possible sources of the inherited zircons from volcano-plutonic and (meta)sedimentary rocks older than 1900 Ma of the Ventuari-Tapajós (or Tapajós-Parima) Province

Domain	Reference number	Rock type	Lithostratigraphic Unit	Age (Ma)	Interpretation	Reference	Method
Central Guyana Domain							
CG4	14	Leucogranite	S-type Taiano Granite	2047 ± 7 2072 ± 3	Late-Transamazonian	CPRM (2003)	D
	–	Taiano Paragneiss	Cauarane Group	2038 ± 17 2074 ± 15	Late-Transamazonian	CPRM (2003)	D
				2223 ± 19	Early-Transamanzonian	Gaudette et al. (1996)	C
CG3	9	Vilhena Mylonite	Rio Urubu "I-type" gneisses	2145 ± 5	Early-Transamanzonian	CPRM (2003)	D
Surumu Domain							
	–	Uiramutã Quartz sandstone	Arai Formation (Roraima Supergroup)	1958 ± 19	Pedra Pintada/Surumu	Santos et al. (2003b)	D
				2123 ± 14	Early-Transamanzonian		
				2718 ± 18	Archean		
S1	17	Uraricáa Rhyodacite	Surumu Group	2027 ± 32	Late-Transamazonian	Santos (2002)	D
	16	Surumu Rhyodacite	Surumu Group	2163 ± 10	Early-Transamanzonian		
Parima Domain							
P	–	Uatatás Quartzite	Parima Group	1971 ± 9	Pedra Pintada/Surumu	Santos et al. (2003c)	D
				2098 ± 16	Late-Transamazonian		
				2201 ± 10	Early-Transamanzonian		
				2781 ± 6	Archean		
				2872 ± 6	Archean		
Uatumã-Anauá Domain							
UA2	23	S-type monzogranite (mf156)	S-type Serra Dourada Granite	2138 ± 11	Early-Transamanzonian	This paper	B
UA1	22	Leucogranite (MA246C2)	Blobs and lenses of leucogranite	1959 ± 5	Martins Pereira	This paper	B
				1997 ± 8	Anauá?		
				2128 ± 3	Early-Transamanzonian		
				2354 ± 6	Siderian		
Tapajós Domain							
T1	34	JL Monzogranite	Creporizão Suite	2003 ± 5	Cuiú-Cuiú	Santos et al. (2001)	D
T3	41	Trachyte	Vila Riozinho Volcanic Rocks	2852 ± 4	Archean	Lamarão et al. (2002)	B
				2591 ± 3	Late Archean		
T5	47	Ouro Roxo Andesite	Cuiú-Cuiú Complex	2040 ± 5	Late-Transamazonian	Santos et al. (2001)	D
	50	Cuiú-Cuiú Meta-tonalite	Cuiú-Cuiú Complex	2056 ± 7	Late-Transamazonian		
	48	JL Tonalite	Cuiú-Cuiú Complex	2046 ± 5	Late-Transamazonian		
				2100 ± 7	Early-Transamanzonian		
				2380 ± 8	Siderian		
				2483 ± 19	Siderian		

Notes: (A) Pb-evaporation on single filament; (B) Pb-evaporation on double filament; (C) U–Pb ID-TIMS; (D) U–Pb SHRIMP. Reference number 1–50 and symbols GC1-T5 are the same as in Fig. 12.

(c) The 2354 ± 6 Ma (Siderian, group I) and 2134 ± 15 Ma (Sthaterian, group II) ages suggest local inheritance from older crust (not outcropping), respectively related to the pre-Transamazonian and Transamazonian magmatic events. Transamazonian rocks with 2.26–2.01 Ga (Santos et al., 2003a) have been described ~600 km northeast from the sampled site, in the Maroni-Itacaiúnas or

Transamazon Province (Fig. 1). Transamazonian rocks mainly occur in Brazil (Amapá State; Avelar et al., 2001; Rosa-Costa et al., 2003), French Guyana (Vanderhaeghe et al., 1998; Delor et al., 2003), São Luis Craton (Klein and Moura, 2001) and (its extension) in the West Africa craton (Boher et al., 1992; Milési et al., 1992; Gasquet et al., 2003). In the last case, they are related to Birimian (2185–2150 Ma) and Bandamian (2115–2100 Ma) events.

In West Africa, pre-Birimian ages (Burkinian, according to Lemoine et al., 1990) are described by Gasquet et al. (2003) in Dabakala (Ivory Coast). The 2312 ± 17 Ma age has seen two interpretations by the previously mentioned authors. The first interpretation considers this age representing an Archean inheritance (and not Siderian) based on the complex model of Pb loss in the analyzed zircon crystals. The second interpretation holds that this age is related to the *ca.* 2.3 Ga pre-Birimian crust. According to these authors, the second hypothesis is more consistent due to the systematically well-defined age patterns, around 2.2–2.3 Ga (without evidence of older Archean ages). This second hypothesis gains additional support from the fact that these rocks are not spatially close to the Archean nucleus.

The Siderian age in Uatumã-Anauá Domain (Tapajós-Parima Province) is the first zircon data reported in any section of the central-western Guyana Shield and suggest probably contamination-assimilation of older country rocks with pre-Transamazonian and post-Archean ages, not exposed in surface. The proximity with Central Amazonian Province (older than 2.3 Ga) is uncertain, because provincial boundaries are not precise. Although Siderian-Neoarchean Nd model ages are describe in the central Guyana Shield (e.g. Faria *et al.*, 2002; Costa, 2005), this province remains poorly investigated, while U–Pb and Pb–Pb geochronological data are scarce, showing ages systematically lower than 2.3 Ga.

Other Siderian ages have been found in the Amazonian Craton, but not in the Guyana Shield. Additionally, the Siderian age (2354 Ma) in Uatumã-Anauá is lower than the Siderian inheritance (2380–2483 Ma) obtained by Santos et al. (2001) in Cuiú-Cuiú rocks from the Tapajós Domain (Brazil Central Shield). Other Siderian ages are reported in the Transamazonian terrane (2.20–1.99 Ga, Vasquez et al., 2003) of Bacajá domain (to north–northwest of Carajás Province) where zircon dating from Vasquez et al. (2003), Santos et al. (in Faraco et al., 2003), and Macambira et al. (2004) yielded 2.44–2.30, 2.47–2.31 and 2.36 Ga, respectively.

7. Tapajós and Uatumã-Anauá domains: chronostratigraphy and implications for geological evolution of the Tapajós-Parima or Ventuari-Tapajós provinces

Previous and new geochronological data have shown several similarities among granitoid rocks from the Northern Uatumã-Anauá Domain and Tapajós Domain (orogenic subdomain, CPRM, 2000b) (Tables 5 and 6). The Orosirian primitive arc inliers, for example, are represented by the Anauá Northern Uatumã-Anauá Domain and Cuiú-Cuiú (Tapajós) TTG-like complexes and are the oldest rocks outcropping in these regions.

In Northern Uatumã-Anauá Domain, the Anauá Tonalite is 2028 ± 9 Ma old (Table 5; Fig. 12), but does not have inheritance evidence and shows εNd of −0.20. This is interpreted as being of juvenile origin (Faria et al., 2002), although only one sample had been analyzed. The Cuiú–Cuiú Complex of the Tapajós Domain shows an age range of 2033–2005 Ma and the older types are coeval to the Anauá granitoid rocks from the Northern Uatumã-Anauá Domain (Table 5; Fig. 12). In contrast to Anauá types, the Cuiú–Cuiú Complex yields several inherited zircon components (Table 6; Fig. 12), in which, the main inheritance is from Transamazonian (2040–2100 Ma), with minor Siderian to Archean records (2380–2483 Ma).

The well-defined interval age of Martins Pereira Granite (1980–1969 Ma) in the Northern Uatumã-Anauá Domain is also very similar to that shown by the Creporizão Suite (1980–1951 Ma) from the Tapajós Domain (Table 5; Fig. 12; CPRM, 2000b; Santos et al., 2000, 2001). Similarly, the Old São Jorge Granite (Lamarão et al., 2002) of the Tapajós Domain is c. 10 Ma older than the Creporizão Suite, but both high-K calc-alkaline granites are related to the Creporizão Orogeny (1.98–1.96 Ga), according to Santos et al. (2004). The Pedra Pintada granitoid rocks (Fraga et al., 1996) in the Surumu Domain (Orocaima event, Reis et al., 2000) are also probably coeval (1958 Ma, CPRM, 2003) to the calc-alkaline Martins Pereira Granite.

In Northern Uatumã-Anauá Domain, lenses of leucosyenogranite are ∼70 m.y. younger than the Martins Pereira host-rock and show crystallization age (1906 ± 4 Ma) similar to those of the Igarapé Azul-Caroebe granitoid rocks (Água Branca magmatism: 1906–1885 Ma) describe in the Southern Uatumã-Anauá Domain. Some similar inherited ages are also observed in both granitic types, such as Martins Pereira (meta)granitoid rocks and Transamazonian inheritances (Table 6), whereas Siderian inheritance is restrict to the leucogranites. The same 1.90–1.88 Ga age interval cor-

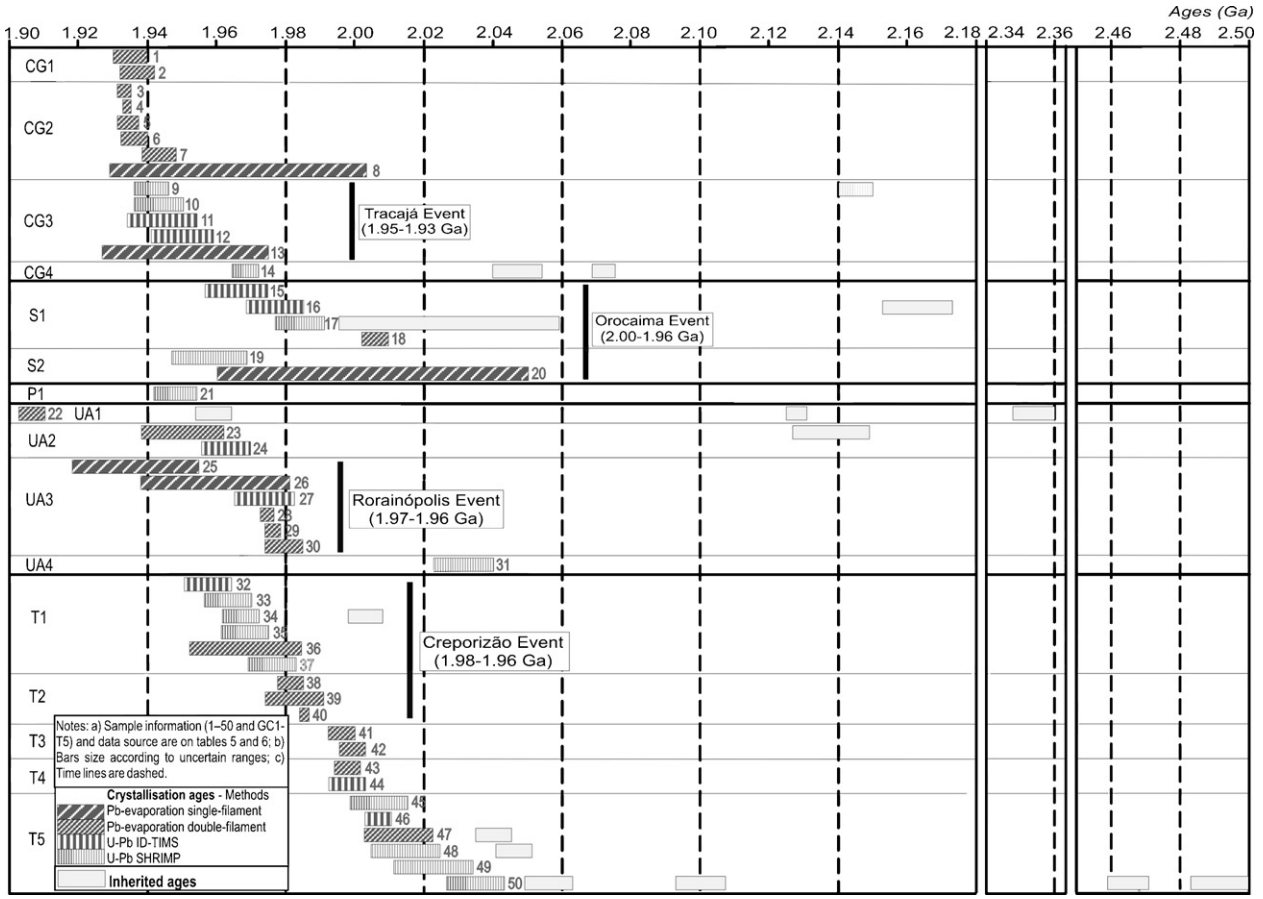

Fig. 12. Temporal distribution of main magmatic rocks older than 1900 Ma of Ventuari-Tapajós (or Parima-Tapajós) Province, grouped by geological domains: CG, Central Guyana; S, Surumu; P, Parima; UA, Uatumã-Anauá; T, Tapajós.

responds also to the Tropas and Parauari magmatism, in the Tapajós Domain (Table 5).

In contrast with Roraima region – where the S-type granites (*e.g.* Serra Dourada, Curuxuim and Amajari), granulites (*e.g.* Barauana) and charnockites are relatively common – these rock types are scarce in the Tapajós Domain. They are locally described as small garnet leucogranite bodies (not mapped on the 1:250,000 scale) associated with Cuiú-Cuiú metagranitoid rocks (Almeida et al., 2001) and have not been dated previously. The scarcity of S-type granites and granulite metamorphism suggests that the collisional processes were less intense in the Tapajós Domain.

8. Conclusions

Geological, geochronological and geochemical data available for granitoid rocks from southeastern Roraima (Brazil) suggest Paleoproterozoic evolution in at least two stages: the Anauá orogeny is related to 2.03 Ga TTG granitoid rocks (*accretionary phase* generating the Anauá granitoid rocks and Cauarane metavolcanosedimentary cover), followed by crustal thickening and anatexis around 1.97–1.96 Ga (*collisional phase* generating Martins Pereira and Serra Dourada granites). A juvenile origin is envisaged for Anauá rocks, but scarce Nd isotopic data do not make this hypothesis conclusive. The Northern Uatumã-Anauá Domain crust, characterized by Orosirian granitoid rocks, is mainly thought to have been generated by reworking of older Transamazonian and minor Siderian crust, according to inherited zircon records.

The following magmatic events can be listed as had occurred for the Northern Uatumã-Anauá Domain:

(A) 2.03 Ga—Crystallization of Anauá Tonalite within the TTG association, representing a primitive arc (?) in southeastern Roraima with related back arc basins.

(B) 1.97–1.96 Ga—Martins Pereira high-K calc-alkaline (meta)granitoid rocks and Serra Dourada S-type granite showing similar crystallization ages. These rocks are probably related to crustal thickening and anatexis in the latest (or after) stage of Anauá arc evolution.
(C) *ca.* 1.90 Ga—meter to centimeter scale leucogranite blobs and lenses (low degree of partial melting?). It is thought that these pods in-filled older, planar structures in the Martins Pereira (meta)granitoid rocks. A regional-scale magmatic event (1.90–1.89 Ga) is mentioned in the southern Uatumã-Anauá Domain, and is believed to be related to the Igarapé Azul and Água Branca granitoid rocks and coeval volcanism (Almeida *et al.*, 2002; Almeida and Macambira, 2003).

Furthermore, possibly two main periods are also recorded in inherited zircon:

(A) Siderian (2.35 Ga)—only one zircon crystal with this age was detected in the lenses of leucogranite, but it represents the first indication of Siderian crust (host-rock or material source) in the central Guyana Shield. Alternatively, this Siderian age could be the result of an isotopic mixing between "Transamazonic" and "Archean" components of the same zircon or partial resetting of an older grain. On the other hand, similar ages are also recorded in West Africa craton (2312 Ma, Gasquet et al., 2003), Bacajá (2359 ± 3 Ma, Macambira et al., 2004) and Tapajós domains (2483–2380 Ma, Santos et al., 2001) in Amazonian craton.
(B) Rhyacian (2.14–2.13 Ga, Transamazonian event)—this age interval is yielded by the oldest zircon crystals from the Serra Dourada S-type granite (two crystals) and group II from the lenses of leucogranite (three crystals). Similar inheritance (2163–2100 Ma) was observed in Surumu, Central Guyana and Tapajós domains (CPRM, 2003; Santos et al., 2001, 2003b).

Neoarchean inheritance is not recorded in the Northern Uatumã-Anauá Domain, but is recorded locally in other domains of Tapajós-Parima Province, such as Tapajós (2852–2591 Ma, Lamarão et al., 2002) and Parima (2872–2781 Ma, Santos et al., 2003c) domains.

Previous studies have recognized three geochronological provinces in southeastern Roraima, but new geological, geochronological and geochemical data presented here shows that this region is very similar to the Tapajós Domain (Santos et al., 2004) and reinforce the Ventuari-Tapajós or Parima-Tapajós provinces prolongation in southeastern Roraima, taking into account that rocks older than 2.03 Ga are not exposed in the studied region. However, the Central Amazonian and Maroni-Itacaiúnas provinces seem to be important crustal sources for the rocks of the Northern Uatumã-Anauá Domain, suggesting partial or total crustal recycling.

In summary, the I-type high-K calc-alkaline Martins Pereira (meta)granitoid rocks and S-type Serra Dourada granites were generated in the Northern Uatumã-Anauá Domain (Ventuari-Tapajós or Tapajós-Parima provinces), probably during amalgamation of TTG-like Anauá magmatic arc (2028 Ma) with Transamazon (2.2–2.0 Ga) and Central Amazonian (older than 2.3 Ga) terranes.

Some authors argue that most collision orogenic systems have a prior accretion history (*e.g.* Van Staal et al., 1998), so it is easy to confuse the accretion and collision histories in ancient examples, such as the Ventuari-Tapajós or Tapajós-Parima provinces. This makes it difficult to rebuild the Anauá orogeny and the hypothesis presented in this paper is only a first approach of the tectonic evolution of the central portion of the Guyana Shield.

Acknowledgments

Special thanks to the colleagues of CPRM (Geological Survey of Brazil) and Sérgio C. Valente (UFRuRJ), Claúdio M. Valeriano (UERJ), Cândido A.V. Moura and Claúdio N. Lamarão (UFPA) for discussions and Nicholas Tailby (Australian National University) for the English review. The authors are also grateful to CPRM-Geological Survey of Brazil for the research grants and FINEP (CT-Mineral 01/2001 Project) and Isotope Geology Laboratory of Federal University of Pará for support of laboratorial work. Thanks also to the two anonymous referees for suggestions to the manuscript.

References

Almeida, M.E., Macambira, M.J.B., 2003. Aspectos geológicos e litoquímicos dos granitóides cálcio-alcalinos Paleoproterozóicos do sudeste de Roraima. In: SBGq, Cong. Brasil. Geoq., vol. 9, Anais, pp. 775–778 (in Portuguese).

Almeida, M.E., Fraga, L.M.B., Macambira, M.J.B., 1997. New geochronological data of calc-alkaline granitoids of Roraima State, Brazil. In: IG/USP, South-American Symposium on Isotope Geology, vol. 1, pp. 34–37 (Abstract).

Almeida, M.E., Brito, M.F.L., Ferreira, A.L., Monteiro, M.A.S., 2001. Evolução Tectono-estrutural da região do médio-alto curso do rio Tapajós. In: Reis, N.J., Monteiro, M.A.S. (Orgs.), Contribuições à Geologia da Amazônia, vol. 2. Belém, SBG, pp. 57–112. (in Portuguese).

Almeida, M.E., Macambira, M.J.B., Faria, M.S.G. de, 2002. A Granitogênese Paleoproterozóica do Sul de Roraima. In: SBG, Congresso Brasileiro de Geologia, vol. 41, Anais, p. 434 (in Portuguese).

Altherr, R., Holl, A., Hegner, E., Langer, C., Kreuzer, H., 2000. High-potassium, calc-alkaline I-type plutonism in the European Variscides: northern Vosges (France) and northern Schwarzwald (Germany). Lithos 50, 51–73.

Andsell, K.M., Kyser, T.K., 1991. Plutonism, deformation and metamorphism in the Proterozoic Flin Flon greenstone belt, Canada: Limits on timing provided by single-zircon Pb-evaporation technique. Geology 19, 518–521.

Avelar, V.G. de, Lafon, J.-M., Delor, C., 2001. Geocronologia Pb-Pb em zircão e Sm-Nd em rocha total da porção centro-norte do Amapá. Implicações para a evolução geodinâmica do Escudo das Guianas. In: SBG, Simpósio de Geologia da Amazônia, vol. 7, Belém, Resumos Expandidos (CD-ROM) (in Portuguese).

Barbarin, B., 1999. A review of the relationships between granitoid types, their origins and their geodynamic environments. Lithos 46, 605–626.

Barker, F., Farmer, G.L., Ayuso, R.A., Plafker, G., Lull, J.S., 1992. The 50 Ma granodiorites of the eastern Gulf of Alaska: melting in an accretionary prism in the forearc. J. Geophys. Res. 97, 6757–6778.

Boher, M., Abouchami, W., Michard, A., Albarède, F., Arndt, N., 1992. Crustal growth in West Africa at 2.1 Ga. J. Geophys. Res. 97, 345–369.

Bonin, B., 1990. From orogenic to anorogenic settings: evolution of granitoid suites after a major orogenesis. Geol. J. 25, 261–270.

Boynton, W.V., 1984. Cosmochemistry of the rare earth elements: meteorite studies. In: Henderson, P. (Ed.), Rare Earth Element Geochemistry. Elsevier Publ., pp. 63–114.

Brown, G.C., Thorpe, R.S., Webb, P.C., 1984. The geochemical characteristics of granitoids in contrasting arcs and comments on magma sources. J. Geol. Soc. Lond. 141, 413–426.

Chappell, B.W., White, A.J.R., 1992. I- and S-type granites in the Lachlan Fold Belt. Trans. R. Soc. Edinburg: Earth Sci. 83, 1–26.

Cordani, U.G., Tassinari, C.C.G., Teixeira, W., Basei, M.A.S., Kawashita, K., 1979. Evolução tectônica da Amazônia com base nos dados geocronológicos. In: Congresso Geológico Chileno, vol. 2, Arica, Anais, v.4, pp. 137–148 (in Portuguese).

Costa, J.A.V., Costa, J.B.S., Macambira, M.J.B., 2001. Grupo Surumu e Suíte Intrusiva Saracura, RR - Novas Idades Pb-Pb em Zircão e Interpretação Tectônica. In: SBG, Simpósio de Geologia da Amazônia, vol. 7, Belém, Pará, Resumos Expandidos, CD-ROM, pp. 16–19 (in Portuguese).

Costa, S. dos S. 2005. Análise integrada dos dados geofísicos, geológicos e de sensoriamento remoto do Cinturão Guiana Central e áreas adjacentes do estado de Roraima. Doctoral thesis, Unicamp, São Paulo, 157 p. Unpublished. (abstract in English).

Cox, K.G., Bell, J.D., Pankhurst, R.J., 1987. The Interpretation of Igneous Rocks, fifth ed. George Allen and Unwin Ltd., London, p. 450.

CPRM, 1999. Programa Levantamentos Geológicos Básicos do Brasil. Roraima Central, Folhas NA.20-X-B e NA.20-X-D (integrais), NA.20-X-A, NA.20-X-C, NA.21-V-A e NA.21-V-C (parciais). Escala 1:500.000. Estado de Roraima. Manaus, CPRM, p. 166 [CD-ROM] (in Portuguese).

CPRM, 2000a. Programa Levantamentos Geológicos Básicos do Brasil. Caracaraí, Folhas NA.20-Z-B e NA.20-Z-D (integrais), NA.20-Z-A, NA.21-Y-A, NA.20-Z-C e NA.21-Y-C (parciais). Escala 1:500.000. Estado de Roraima. Manaus, CPRM, p. 157 [CD-ROM] (abstract in English).

CPRM, 2000b. Programa Levantamentos Geológicos Básicos do Brasil. Projeto Especial Província Mineral do Tapajós. Geologia e Recursos Minerais. Vila Riozinho, Folha SB.21-Z-A. Escala 1:250.000. Estado do Pará. Nota Explicativa. CPRM/Serviço Geológico do Brasil [CD-ROM] (in Portuguese).

CPRM, 2003. Programa Levantamentos Geológicos Básicos do Brasil. Geologia, Tectônica e Recursos Minerais do Brasil: sistema de informações geográficas—SIG. Rio de Janeiro: CPRM, 2003. Mapas Escala 1:2.500.000. 4 CDs ROM (abstract in English).

CPRM, 2005. Programa Levantamentos Geológicos Básicos do Brasil. Mapa Geológico do Brasil. Escala 1:1000.000. 41 mapas Brasília, MME. Edição 2004 [CD-ROM] (in Portuguese).

CPRM, 2006. Programa Integração, Atualização e Difusão de Dados da Geologia do Brasil: Subprograma Mapas Geológicos Estaduais. Geologia e Recursos Minerais do Estado do Amazonas. Manaus, CPRM/CIAMA-AM, 2006. Escala 1:1.000.000. Texto explicativo, p. 148 [CD-ROM] (in Portuguese).

Daly, S.J., Fanning, C.M., Fairclough, M.C., 1998. Tectonic evolution and exploration potential of the Gawler Craton, South Australia. AGSO J. Aust. Geol. Geophys. 17, 145–168.

Daly, J.S., Balagansky, V.V., Timmerman, M.J., Whitehouse, M.J., de Jong, K., Guise, P., Bogdanova, S., Gorbatschev, R., Bridgewater, D., 2001. Ion microprobe U–Pb zircon geochronology and isotopic evidence for a trans-crustal suture in the Lapland–Kola Orogen, northern Fennoscandian Shield. Pecamb. Res. 105, 289–314.

Delor, C., Lahondère, D., Egal, E., Lafon, J.-M., Cocherie, A., Guerrot, C., Rossi, P., Truffert, C., Théveniaut, H., Phillips, D., Avelar, V.G. de, 2003. Transamazonian crustal growth and reworking as revealed by the 1:500,000-Scale geological map of French Guiana. In: Géologie de la France, vol. 2–4, second ed., pp. 5–57.

Dougherty-Page, J.S., Bartlett, J.M., 1999. New analytical procedures to increase the resolution of zircon geochronology by the evaporation technique. Chem. Geol. 153, 227–240.

Faraco, M.T.L., Vale, A.G., Santos, J.O.S. dos, Luzardo, R., Ferreira, A.L., Oliveira, M.A., Marinho, P.A.C., 2003. Levantamento geológico na região a norte do Bloco Carajás: Notícias preliminares. In: SBG, Simpósio de Geologia da Amazônia, vol. 8, Manaus, AM, Anais [CD-ROM] (in Portuguese).

Faria, M.S.G. de, Luzardo, R., Pinheiro, S.S., 1999. Litoquímica e petrogênese do Granito Igarapé Azul. In: SBG, Simpósio de Geologia da Amazônia, vol. 6, Anais, pp. 577–580 (in Portuguese).

Faria, M.S.G. de, Santos, J.O.S. dos, Luzardo, R., Hartmann, L.A., McNaughton, N.J., 2002. The oldest island arc of Roraima State, Brazil—2.03 Ga: zircon SHRIMP U–Pb geochronology of Anauá Complex. In: SBG, Congresso Brasileiro de Geologia, vol. 41, Anais, p. 306.

Fraga, L.M.B., 2002. A Associação Anortosito–Mangerito–Granito Rapakivi (AMG) do Cinturão Güiana Central, Roraima e Suas Encaixantes Paleoproterozóicas: Evolução Estrutural, Geocronologia e Petrologia. CPGG, UFPA, Tese de Doutorado, p. 386 (inédito) (in Portuguese).

Fraga, L.M.B., Reis, N.J., Araújo, R.V., Haddad, R.C., 1996. Suíte Intrusiva Pedra Pintada—Um Registro do Magmatismo Pós-colisional no Estado de Roraima. In: SBG, Simpósio de Geologia da Amazônia, vol. 5, Belém, PA. Anais, pp. 76–78 (in Portuguese).

Fraga, L.M.B., Almeida, M.E., Macambira, J.B., 1997. First lead-lead zircon ages of charnockitic rocks from Central Güiana Belt (CGB) in the state of Roraima, Brazil. In: South-American Symposium on Isotope Geology, Campos do Jordão, Resumo, pp. 115–117.

Fraga, L.M.B., Macambira, M.J.B., Dall'Agnol, R., Costa, J.B.S., 2003. The age of the charnockitic rocks of the Serra da Prata Intru-

sive Suite, Central Guyana Belt, Guyana Shield. In: SBG, Simpósio de Geologia da Amazônia, vol. 8, Manaus, AM, Anais, (CD-ROM).

Gasquet, D., Barbey, P., Adoua, M., Paquette, J.L., 2003. Structure, Sr–Nd isotope geochemistry and zircon U–Pb geochronology of the granitoids of the Dabakala area (Cote d'Ivoire): evidence for a 2. 3 Ga crustal growth event in the Palaeoproterozoic of West Africa? Precamb. Res. 127, 329–354.

Gaudette, H.E., Olszewski Jr., W.J., Santos, J.O.S.dos., 1996. Geochronology of Precambriam rocks from the northern part of Güiana Shield, State of Roraima, Brazil. J. S. Am. Earth Sci. 9, 183–195.

Klein, E.L., Moura, C.A.V., 2001. Age constrains on the granitoids and metavolcanics rocks of the São Luís Craton and Gurupi Belt, Northern Brazil: Implications for lithostratigraphy and geological evolution. Intern. Geol. Rev. 43, 237–253.

Klötzli, U.S., 1999. Th/U zonation in zircon derived from evaporation analysis: a model and its implications. Chem. Geol. 158, 25–333.

Kober, B., 1986. Whole grain evaporation for $^{207}Pb/^{206}Pb$ age investigations on single zircons using a double filament source. Contrib. Miner. Petrol. 93, 82–490.

Kober, B., 1987. Single-grain evaporation combined with Pb + emitter bedding for $^{207}Pb/^{206}Pb$ investigations using thermal ion mass spectrometry, and implications for zirconology. Contrib. Miner. Petrol. 96, 63–71.

Krymsky, R., 2002. Metodologia de análise de U–Pb em mono zircão com traçador ^{235}U-^{205}Pb. Universidade Federal do Pará, Laboratório de Geologia Isotópica, p. 7 (in Portuguese).

Lamarão, C.N., Dall'Agnol, R., Lafon, J.-M., Lima, E.F., 2002. Geology, geochemistry and Pb–Pb zircon geochronology of the Paleoproterozoic magmatism of Vila Riozinho, Tapajós gold province, Amazonian craton. Brazil. Precamb. Res. 119 (1–4), 189–223.

Lemoine, S., Tempier, P., Bassot, J.-P., Caen-Vachette, M., Vialette, Y., Toure, S., Wenmenga, U., 1990. The Burkinian, an orogenic cycle, precursor of the Eburnean. Geol. J. 25, 171–188.

Ludwig, K.R., 1999. Using ISOPLOT/Ex, Version 2: A Geochronological Toolkit for Microsoft Excel. Berkeley Geochronological Center Special Publication Ia, p. 47.

Macambira, M.J.B., Scheller, T., 1994. Estudo comparativo entre métodos geocronológicos aplicados em zircões: o caso do Granodiorito Rio Maria. In: Simpósio de Geologia da Amazônia., vol. 4, Belém, 1994. Bol. Res. Exp., Belém/SBG, pp. 343–346.

Macambira, M.J.B., Almeida, M.E., Santos, L.S., 2002. Idade de Zircão das Vulcânicas Iricoumé do Sudeste de Roraima: contribuição para a redefinição do Supergrupo Uatumã. In: SBG, Simpósio Sobre Vulcanismo Ambientes Associados, vol. 2, Anais, p. 22 (in Portuguese).

Macambira, M.J.B., Silva, D.C.C., Vasquez, M.L., Barros, C.E.M., 2004. Investigação do limite arqueano-paleoproterozóico ao norte da Província de Carajás, Amazônia Oriental. In: Congresso Brasileiro de Geologia, vol. 42, Araxá, Anais, (CD-ROM).

Maniar, P.D., Piccoli, P.M., 1989. Tectonic discrimination of granitoids. Geol. Soc. Am. Bull. 101, 635–643.

McDonough, M.R., Grover, T.W., McNicoll, V.J., Lindsay, D.D., 1993. Preliminary geology of the southern Taltson magmatic zone, Canadian Shield, northeastern Alberta. Geol. Surv. Can. Pap. 93-1C, 221–231.

Milési, J.P., Ledru, P., Feybesse, J.L., Dommanget, A., Marcoux, E., 1992. Early Proterozoic ore deposits and tectonics of the Birimian orogenic belt. West Afri. Precamb. Res. 58, 305–344.

Patiño-Douce, A.E., 1996. Effects of pressure and H_2O content on the composition of primary crustal melts. Trans. R. Soc. Edinburgh: Earth Sci. 87, 11–21.

Patiño-Douce, A.E., 1999. What do experiments tell us about the relative contributions of crust and mantle to the origin of granitic magmas? In: Castro, A., Fernandez, C., Vigneressese, J.L. (Eds.), Understanding Granites: Integrating New and Classical Techniques, vol. 168. Geol. Soc. Lond., Special Publication, vol. 168, pp. 55–75.

Patiño-Douce, A.E., Beard, J.S., 1996. Effects of P, fO_2 and Mg/Fe ratio on dehydration melting of model metagreywackes. J. Petrol. 37, 999–1024.

Pearce, J.A., 1996. Sources and settings of granitic rocks. Episodes 19, 120–125.

Pearce, J.A., Harris, N.B., Tindle, A.G., 1984. Trace element discrimination diagrams for the tectonic interpretation of granitic rocks. J. Petrol. 25, 956–983.

Peccerillo, A., Taylor, S.R., 1976. Geochemistry of Eocene calc-alkaline rocks from Kastamonu area, Northern Turkey. Contrib. Miner. Petrol. 58, 63–81.

Pupin, J.P., 1980. Zircon and granite petrology. Contrib. Miner. Petrol. 73, 207–220.

Reis, N.J., Faria, M.S.G.de, Fraga, L.M.B., Haddad, R.C., 2000. Orosirian calc-alkaline volcanism and the orocaima event in the Northern Amazonian Cráton, Eastern Roraima State. Brazil. Rev. Bras. Geoc. 30 (3), 380–383.

Reis, N.J., Fraga, L.M.B., Faria, M.S.G. de, Almeida, M.E., 2003. Geologia do Estado de Roraima. In: Géologie de la France, vol. 2–4, pp. 71–84 (in Portuguese).

Rickwood, P., 1989. Boundary lines within petrologic diagrams which use oxides of major and minor elements. Lithos 22, 247–263.

Roberts, M.P., Clemens, J.D., 1993. The origin of high-K, calc-alkaline, I-type granitoid magmas. Geology 21, 825–828.

Rosa-Costa L.T., Ricci P.S.F., Lafon J.M., Vasquez M.L., Carvalho J.M.A., Klein E.L., Macambira, E.M.B., 2003. Geology and geochronology of Archean and Paleoproterozoic domains of the southwestern Amapá and Northwestern Pará, Brazil, southeastern Guiana Shield. Géologie de la France, vol. 2–4, pp. 101–120.

Santos, J.O.S. dos, 2002. Field Workshop: Manaus (AM)-Pacaraima (RR) Transect. GIS Brasil Program. CPRM, Manaus, Internal Report (in Portuguese).

Santos, J.O.S.dos, Olszewski, W., 1988. Idade dos granulitos tipo Kanuku em Roraima. In: SBG/DNPM, Congresso Latino-Americano de Geologia, vol. 7, Belém, Anais, pp. 378–388 (in Portuguese).

Santos, J.O.S. dos, Silva, L.C., Faria, M.S.G. de, Macambira, M.J.B., 1997. Pb-Pb single crystal, evaporation isotopic study on the post-tectonic, sub-alkalic, A-type Moderna granite, Mapuera intrusive suite, State of Roraima, northern Brazil. In: SBG, Symposium of Granites and Associated Mineralizations, vol. 2, pp. 273–275 (Extended Abstract and Program).

Santos, J.O.S. dos, Hartmann, L.A., Gaudette, H.E., Groves, D.I., McNaughton, N.J., Fletcher, I.R., 2000. A new understanding of the provinces of the Amazon Craton based on integration of field mapping and U–Pb and Sm-Nd geochronology. Gond. Res. 3 (4), 453–488.

Santos, J.O.S. dos, Groves, D.I., Hartmann, L.A., McNaughton, N.J., Moura, M.B., 2001. Gold deposits of the Tapajós and Alta Floresta domains, Tapajós–Parima orogenic belt, Amazon Craton. Brazil. Mineralium Deposita 36, 278–299.

Santos, J.O., dos, S., Hartmann, L.A., Bossi, J., McNaughton, N.J., Fletcher, I.R., 2003a. Duration of the Trans-Amazon Cycle and

its correlation within South America based on U–Pb SHRIMP geochronology of the La Plata Craton, Uruguay. Intern. Geol. Rev. 45 (1), 27–48.

Santos, J.O.S. dos, Potter, P.E., Reis, N.J., Hartmann, L.A., Fletcher, I.R., McNaughton, N.J., 2003b. Age, source and regional stratigraphy of the Roraima supergroup and Roraima-like Sequences in Northern South America, based on U–Pb geochronology. Geol. Soc. Am. Bull. 115 (3), 331–348.

Santos, J.O.S. dos, Reis, N.J., Chemale, F., Hartmann, L.A., Pinheiro, S.da.S., McNaughton, N.J., 2003c. Paleoproterozoic evolution of Northwestern Roraima State—absence of archean crust, based on U–Pb and Sm–Nd isotopic evidence. In: Simposyum of South-American on Isotope Geology, vol. 4, Pucon, Chile.

Santos, J.O.S. dos, Van Breemen, O.B., Groves, D.I., Hartmann, L.A., Almeida, M.E., McNaughton, N.J., Fletcher, I.R., 2004. Timing and evolution of multiple Paleoproterozoic magmatic arcs in the Tapajós Domain, Amazon Craton: constraints from SHRIMP and TIMS zircon, baddeleyite and titanite U–Pb geochronology. Precamb. Res. 131 (1–2, 10), 73–109.

Santos, J.O.S. dos, Hartmann, L.A., Faria, M.S.G. de, Riker, S.R.L., Souza, M.M. de, Almeida, M.E., McNaughton, N.J., 2006. A Compartimentação do Cráton Amazonas em Províncias: Avanços ocorridos no período 2000–2006. In: SBG, Simpósio de Geologia da Amazônia, vol. 9, Belém, [CD-ROM] (in Portuguese).

Sardinha, A.S., 1999. Petrografia do Granito Igarapé Azul, Sudeste do Estado de Roraima. Trabalho de Conclusão de Curso, UFPA, Belém, p. 32 (in Portuguese).

Scheller, T. 1998. Zircon. DOS Shareware, UFPA, Belém, Pará-Iso.

Schobbenhaus, C., Hoppe, A., Lork, A., Baumann, A., 1994. Idade U/Pb do Magmatismo Uatumã no Norte do Cráton Amazônico, Escudo das Guianas (Brasil): Primeiros Resultados. In: SBG, Congresso Brasileiro de Geologia, vol. 38, Camboriú, Anais, 2, pp. 395–397 (in Portuguese).

Shand, S.J., 1927. Eruptive Rocks. D. Van Nostrand Company, New York, p. 360.

Sheppard, S., Occhipinti, S.A., Tyler, I.M., 2004. A 2005–1970 Ma Andean-type batholith in the southern Gascoyne Complex, Western Australia. Precamb. Res. 128, 257–277.

Söderlund, U., 1996. Convetional U–Pb dating *vs.* single-zircon Pb evaporation dating of complex zircons from a pegmatite in the high-grade gneisses of southwestern Sweden. Lithos 38, 93–105.

Stacey, J.S., Kramers, J.D., 1975. Approximation of terrestrial lead isotope evolution by a two-stage model. Earth Plan. Sci. Lett. 26, 207–221.

Steiger, R.H., Jager, J., 1977. Convention of the use of decay constants in geo- and cosmochronology. Earth Plan. Sci. Lett. 36, 359–362.

Tassinari, C.C.G., 1996. O Mapa Geocronológico do Cráton Amazônico no Brasil: revisão dos dados isotópicos. Tese de Livre docência, Instituto de Geociências da Universidade de São Paulo, p. 139 (in Portuguese).

Tassinari, C.C.G., Macambira, M.J.B., 1999. Geochronological Provinces of the Amazonian Craton. Episodes 22 (3), 174–182.

Tassinari, C.C.G., Macambira, M.J.B., 2004. A Evolução Tectônica do Cráton Amazônico. In: Mantesso-Neto, Virginio, Bartoreli, Andrea, Carneiro, Celso Dal Ré, Brito-Neves, Benjamin Bley de (Eds.), Geologia do Continente Sul-Americano—Evolução da Obra de Fernando Flávio Marques de Almeida, São Paulo, Ed. Beca, pp. 471–485 (in Portuguese).

Teixeira, W., Tassinari, C.C.G., Cordani, U.G., Kawashita, K., 1989. A review of the Geochronology of the Amazonian Craton tectonic implications. Precamb. Res. 42, 213–227.

Thompson, A.B., 1996. Fertility of crustal rocks during anatexis. Trans. R. Soc. Edinburgh Earth Sci. 87, 1–10.

Thuy Nguyen, T.B., Satir, M., Siebel, W., Venneman, T., van Long, T., 2004. Geochemical and isotopic constraints on the petrogenesis of granitoids from Dalat zone, southern Vietnam. J. Asian Earth Sci. 23, 467–482.

Vanderhaeghe, O., Ledru, D., Thiéblemont, D., Egal, E., Cocherie, A., Tegyey, M., Milési, J.P., 1998. Contrasting mechanisms of crustal growth. Geodynamic evolution of the Paleoproterozoic granite-greenstone belts of French Guiana. Precamb. Res. 92, 165–193.

Van Staal, C.S., Dewey, J.F., MacNiocaill, C., McKerrow, W.S., 1998. The Cambrian-Silurian tectonic evolution of the northern Appalachians and British Caledonides: history of a complex, west and southwest Pacific-type segment of Iapetus. In: Blundell, D., Scott, A.C. (Eds.), Lyell: The Past is the Key to the Present. Geol. Soc. London, Special Publication, vol. 143, pp. 199–242.

Vasquez, M.L., Macambira, M.J.B., Galarza, M.A., 2003. Granitóides Transamazônicos da Região Iriri-Xingu—Estado do Pará. In: SBG, Simpósio de Geologia da Amazônia, vol. 8, Manaus, Resumos Expandidos (CD-ROM) (in Portuguese).

Watson, E.B., Harrison, T.M., 1983. Zircon saturation revisited: temperature and composition effects in a variety of crustal magma types. Earth Plan. Sci. Lett. 64, 295–304.

Whalen, J.B., Currie, K.L., Chappell, B.W., 1987. A-type granites: geochemical characteristics, discrimination and petrogenesis. Contrib. Miner. Petrol. 95, 407–419.

Wilson, M., 1991. Igneous Petrogenesis: A Global Tectonic Approach, second ed. Harper Collins Acad, London, p. 466.

Wolf, M.B., Wyllie, J.P., 1994. Dehydration-melting of amphibolite at 10 kbar: the effects of temperature and time. Contrib. Miner. Petrol. 115, 369–383.

Wood, D.A., 1979. A variably veined suboceanic upper mantle*/genetic significance for mid-ocean ridge basalts from geochemical evidence. Geology 7, 499–503.